Optimization of CFRP Joints with Fibre Metal Laminates

Submitted by

Radu – Cristian Dumbravă

Supervised by

Lucas Filipe Martins da Silva

Co-supervised by

Ricardo João Camilo Carbas

Abstract

The use of composite materials in industry is growing due to various technological advances in composite materials accompanied by improvements in the structural adhesives used to bond them. Fibre metal laminates (FMLs) are hybrid composite structures based on thin sheets of metal alloys and plies of fibre reinforced by polymeric materials. The fibre/metal composite technology combines the advantages of metallic materials (high bearing strength, impact resistance and reparability characteristics) and fibre reinforced matrix systems (high strength and stiffness, fatigue and corrosion characteristics). Due to their advantages, FMLs are finding great use in many aerospace applications.

The aim of the present project is to use a concept similar to that used in FML to increase the peel strength of composite materials and increase the joint strength of composite adhesive joints. Carbon fibre reinforced plastic (CFRP) composites will be modified by including one or several aluminium sheets during the laminate manufacture to enhance the composite through the thickness properties. The objective is to identify the joint configuration that gives the best joint strength improvement in relation to the CFRP only reference joint.

Finally, experimental and numerical studies have been undertaken on modified CFRP joints to investigate the joint strength of different lay-up solutions and an optimised joint that prevents delamination of adherends was analysed using the finite element method.

Rezumat

Utilizarea materialelor compozite este în continuă creștere, datorită avansării tehnologiei materialelor compozite, precum și a îmbunătățirii continue a adezivilor structurali utilizați pentru a le asambla. Fibre metal laminates (FMLs) sunt compozite hibride, produse utlizând foi metalice subțiri și lamine compuse din rășini armate cu fibre. Materiale compozite tip sandviș metal / rășini armate cu fibre benficiază de avantajele materialelor metalice (rezistență mecanică ridicată, bune caracteristici pentru impact și ușurința în repararea acestora) precum și de cele ale materialelor plastice armate cu fibre (rigiditate și rezistență ridicată, bune caracteristici în cazul solicitărilor variabile sau în cazul coroziunii). Datorită acestor avantaje, FML-urile sunt folosite cel mai des în cadrul industriei aerospațială.

Scopul acestui proiect este de a folosi un concept similar celui utilizat în cazul FML-urilor, pentru a îmbunătății rezistența matricei pe direcție transversală, îmbunătățind astfel capacitatea portantă a asamblării cu adeziv. Materialele plastice armate cu fibre de carbon vor fi alterate prin introducerea uneia sau mai multelor foi de aluminiu, în timpul procesului de fabricație, cu scopul îmbunătățirii proprietăților transversale ale compozitului. Obiectivul este acela de a identifica secvența straturilor care oferă cea mai mare îmbunătățire a capacității portante, raportată la cea a unei asamblări, în care aderenții sunt fabricați doar prin utilizarea materialelor plastice armate cu fibre de carbon, asamblare considerată referință.

Pentru a realiza obiectivul asumat, au fost realizate studii experimentale și analize numerice ale asamblărilor adezive, folosind materiale plastice armate cu fibre de carbon, care au fost modificate prin introducerea unor foi de aluminium. În urma simulărilor numerice, a fost determinat un model de asamblare care împiedica delaminarea substratului și mărește capacitatea portantă a asamblării adezive.

Acknowledgements

I would like to thank:

- Professor Lucas da Silva for giving me the opportunity to work under his supervision, for the guidance and advice given which were very important in the development of this thesis;
- Dr. Ricardo Carbas, for his invaluable help during the theoretical and experimental parts of this study and also for being there whenever I needed help;
- The ADFEUP group for all the help they offered me whenever I needed a fresh pair of eyes;
- My home university for giving me the opportunity to enjoy this international learning experience and FEUP for their hospitality;
- My friends for their support;
- Last but not least, to my family for their endless support in making this international learning experience possible.

Contents

List of tables

List of figures

Nomenclature

Acronyms

Al	Aluminium
CFRP	Carbon fibre reinforced plastic
CTE	Linear thermal expansion coefficient
CZE	Cohesive zone elements
CZM	Cohesive zone models
FEA	Finite element analysis
FML	Fibre metal laminate
FRP	Fibre reinforced plastic
PAA	Phosphoric acid anodizing
S_i	Specimen number *i*
SLJ	Single lap joint
2D	Two dimensions
3D	Three dimensions

Symbols

P	Load
δ	Displacement
ε	Strain
τ	Shear stress
σ	Normal stress
E	Young's modulus
E_i	Young's modulus along *i* axis
G	Shear modulus
G_{ij}	Shear modulus in direction *j* on the plane whose normal is in direction *i*
v	Poisson's ratio
v_{ij}	Poisson's ratio that corresponds to a contraction in direction *j* when an extension is applied in direction *i*
l	Overlap length
b	Substrate width
t_a	Adherend thickness
G_{IC}	Fracture energy in mode I
G_{IIC}	Fracture energy in mode II

1 Introduction

1.1 Background and motivation

Decades have passed since the first use of modern composite materials. Due to their unique qualities compared to traditional materials and the high price, they were used mainly in military applications such as fighter aircraft. More recently, commercial applications for composite materials have emerged, triggered off by a gradual reduction in prices and the very good mechanical properties, tested in the military industry.

Nowadays composite materials can be found everywhere. They can be used to manufacture a wide range of products. For example, they are used for bathtubs, in sports gear, in the automotive industry, but mainly in the aerospace industry. The Boeing 787 airliner has a 50% use by weight of composite materials for its primary structure [1].

This achievement was partly due to advances in adhesive bonding technology, which allows the efficient joining of such composite structures.

A type of composites widely used in the aeronautical industry are the fibre metal laminates (FML). Delft University of Technology first developed these materials. Their research found that the fatigue crack growth rates in adhesive bonded sheet materials can be reduced, if they are built up by laminating and adhesively bonding thin sheets of the material, instead of using on one thick monolithic sheet [2]. The FML concept could be extended to reinforce carbon-fibre using metal, which is the research subject of this work.

1.2 Problem definition

The behaviour of composites is highly anisotropic in respect to both stiffness and strength. In the fibre direction, unidirectional composites can be very strong and stiff whereas the transverse and shear properties are much lower. Bonded joints experience peel loading so the composite may fail in transverse tension before the adhesive fails. The composite adherend splits apart locally due to these peel stresses, thereby destroying the shear transfer capacity between the two adherends. Some authors have studied the problem of peel stresses in adhesive joints with composites and found designs to reduce them. For example, da Silva and Adams [3] propose an internal taper and adhesive fillet to reduce the peel stresses. However, an internal taper and fillet are not easy to manufacture. Other more sophisticated techniques have been proposed such as the use the z-pins to reinforce the through the thickness strength of the composite [4,5]. However, the difficult and expensive

manufacture process is a major drawback of this technique. That is why it is important to study adhesive joints with composites and find a reliable method to avoid the interlaminar failures that commonly occur for this material.

1.3 Objectives

The main idea of the present project is to use a concept similar to that used in fibre metal laminates to increase the peel strength of traditional composite materials and hence increase the joint strength of composite adhesive joints.

CFRP composites will be modified by including one or several aluminium sheets during the laminate manufacture to enhance the composite through the thickness properties.

The objective is to identify the joint configuration that gives the best joint strength improvement in relation to the reference joint composed by CFRP substrates only.

1.4 Research methodology

In order to achieve the aim of the thesis the following work was done:

- Literature review;
- Test composites reinforced with metal sheets;
- Develop a finite element model in order to optimise the FML joints.

1.5 Outline of the thesis

The following chapter of this thesis consists of the literature review on adhesive bonding, fibre reinforced plastics, fibre metal laminates and strength prediction of adhesive joints.

In the third chapter it is detailed the manufacturing process employed in order to obtain the specimens. Information and results regarding the surface treatment are also presented in this chapter, which concludes with the optimum surface treatment of the aluminium sheets.

The fourth chapter of this thesis is reserved for the experimental procedure and results. At the end of the chapter a comparison between studied joints is presented.

A numerical analysis using finite element software ABAQUS® was performed in order to develop a model that can be used to analyse configurations that were not manufactured. Additionally, the residual thermal stresses were also analysed in chapter five.

The conclusions of this study are presented in the sixth chapter while the seventh is dedicated to future work suggestions.

2 Literature review

2.1 Fibre reinforced plastics

2.1.1 History and description of fibre reinforced plastics

A technology for producing glass wool was filed for patent number US2133236 A in 1933, by Games Slayter. A resin, which combined with glass wool, would be capable of creating a fibre reinforced plastic was developed by DuPont in 1936. The first direct ancestor of today's polyester resins was created by a company called American Cyanamid in 1942.

Because of their high strength to weight ratio, FRPs are the materials of choice for the aerospace industry, military industry and automotive industry. These materials have the advantage that they can be tailored to the needs of the designer, for example, in closed-end pressure vessels, such as rocket motor cases, the hoop stress is twice the axial stress, so a pattern of fibres which has this property can be created.

Fibre reinforced plastics (FRP) can also be manufactured by chopping fibres and randomly placing them in a resin matrix or by stacking layers, also called laminas, one over the other, with a very precise alignment of the fibres. This lay-up can be tailored to suit the strength needs of the structure. This is possible because of the anisotropic nature of a lamina.

2.1.2 Failure modes and failure mechanics of FRPs

FRPs are composite materials usually composed of an epoxy resin also called matrix and reinforcement fibres (normally fibreglass, carbon or aramid). Due to this complex structure, the failures modes of these materials are more complex than those of isotropic materials. The most common failure modes are presented in Figure 1.

Delamination of the layers is a failure mode which occurs due to high interlaminar stress. This failure mode is characterized by the separation of adjacent laminas of the FRP. This may result from low velocity impact, eccentricities in the structural load path or from out of plane stress. Even in absence of such situations delamination may occur due to compressive loading which causes general or local buckling.

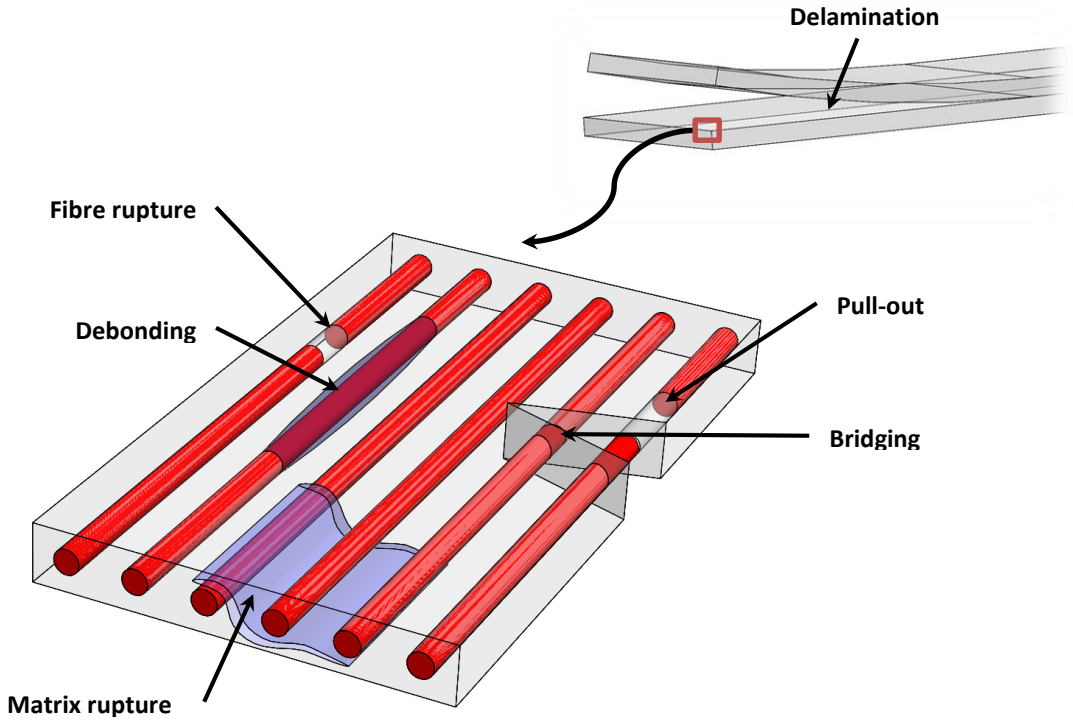

Figure 1 – Failure modes of fibre reinforced plastics

2.2 Fibre metal laminates

FML are a class of hybrid composites, based on thin layers of metals bonded to layers of FRPs. A schematic representation of this concept is presented in Figure 2.

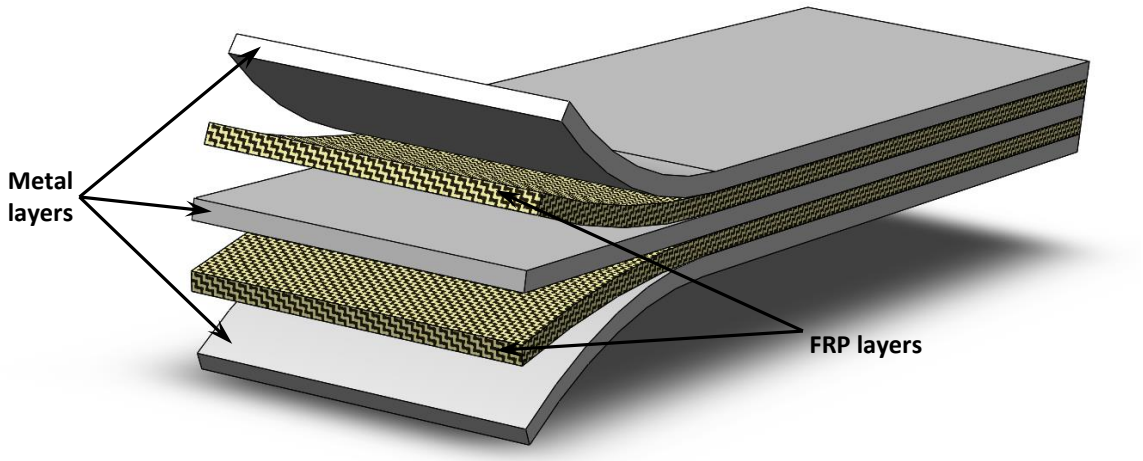

Figure 2 - Schematic representation of a Fibre metal laminate

This type of composite material has seen a strong increase in use in the aerospace industry, and an increasing number of companies have shown interest in replacing

traditional aluminium components with FML [6]. The main objective of this type of stacking is to reinforce the metal alloy.

FML combine the best of two worlds, resulting in a low density composite material with high fatigue resistance, high strength, high fracture toughness and high impact resistance. Besides, these mechanical characteristics also offer better safety than aluminium alone, due to the high melting point of the reinforcing fibres [7].

The first FMLs composites were patented in 1983 (US4500589 A) under the ARALL name [8], which is an abbreviation for "aramid fibre reinforced aluminium laminate". The pilot production of ARALL 1 which is a variant consisting of layers of 7075 aluminium and ARALL 2 which uses 2024 aluminium, was started by the Alcoa Company, after sufficient confidence on the product strength was gained.

In 1990 there was an attempt to improve the ARALL laminates. This consisted in replacing aramid fibres with high strength glass fibres and the resulting material was named GLARE. CFRP is also used to manufacture FMLs but various problems affect this type of composite, known as CARALL. Among these problems are the high thermal stresses, caused by the large mismatch of the coefficient of thermal expansion between CFRP and aluminium and the differences in electrode potential which causes galvanic corrosion. Currently CARALL is only used in limited applications, such as impact absorbers for helicopter struts and aircraft seats [7, 9].

Nowadays FMLs are used extensively in the aerospace industry, for example the upper fuselage panels of the Airbus A380 are manufactured using GLARE, the same material being selected for the bulk cargo floor of the Boeing 777, while ARALL 3 is in production and flight test for the cargo doors of the Boeing C-17.

2.3 Adhesive bonding

According to Kinloch [10], `An adhesive may be defined as a material which when applied to surfaces of materials can join them together and resist separation.' This is a very wide definition, which includes and classifies as adhesives materials not commonly referred to as adhesives such as mortar or solder.

A *structural adhesive* is an adhesive that can resist substantial loads and that is responsible for the strength and stiffness of the structure [11].

2.3.1 Applications of bonded joints

Assembling two parts together is one of the big struggles of mechanical engineers, because a joint has to withstand stresses, has to be light and have very good fatigue properties. Bonded joints have a very good strength to weight ratio and also exhibit good fatigue properties because of their low stress concentration factor.

In the automotive industry using adhesive bonding techniques can reduce the overall mass of a body in white. A car body is responsible for around 40% of the gross weight of a vehicle. Car manufacturers nowadays have to comply with two different design demands. On one side tougher restrictions from the authorities regarding lower CO_2 emissions, which can be obtained by reducing the gross weight of the automobile and on the other side the consumers who want safer cars. The second problem took a normal compact car from around 800 kg (e.g. Volkswagen Golf 1973), to around 1300 kg (e.g. Volkswagen Golf 2005) [12].

The only way to reduce the weight of a car without sacrificing the safety of the passengers or the handling characteristics is by using lighter materials and targeted use of high-strength materials. This leads to the problem of joining dissimilar materials and eliminating the problems regarding galvanic corrosion, stress concentrators due to mechanical fasteners or thermal stresses. The solution to this problem is adhesive bonding, which during the last years gained significant followers in the automotive industry.

In order to better understand this statement a numerical example is given. In 2001 for manufacturing the body of the BMW 7 Series, 10 meters of adhesive bonds were used [13], while the 2011 Mercedes CL-Class has more than 100 meters of adhesive bonds for body in white applications [14]. In addition the all new BMW 7 Series uses CFRP in selected parts in the body structure [15], while the BMW i3 uses a body manufactured completely with composites, an achievement obtained only by using adhesive bonding.

However, in the aerospace and aircraft industry, adhesive bonding is not something new and has been used for at least 30 – 40 years. Modern metallic bonded structures using longitudinal lap joints were first used in commercial aircrafts in the Airbus A300 [16].

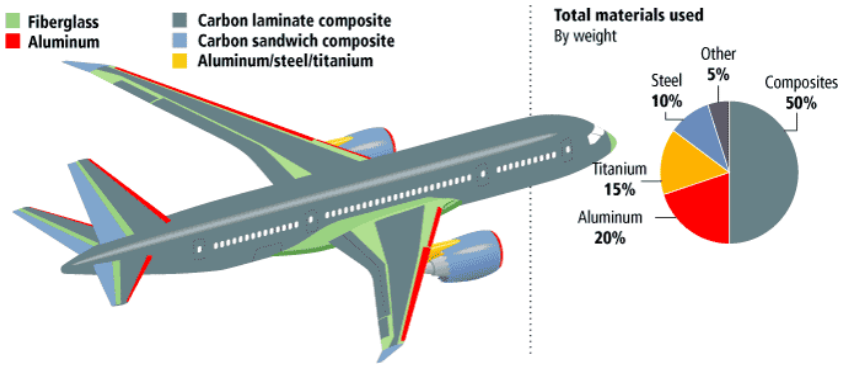

Figure 3 – Materials used in the body structure of the Boeing 787 Dreamliner [17]

For manufacturing of the Boeing 787 Dreamliner's body, composites account for 50% of the weight (Figure 3). To compare, the previous Boeing 777 used only around 12% composites and 50% aluminium.

Adhesive bonding is a crucial technique to repair and maintain these modern aircraft. When a 787 belonging to Ethiopian Airlines suffered fire damage, engineers from Boeing had to find a solution to repair the barrel section, which is a one piece part, manufactured out of CFRP. In order to repair the damage, a crown section was removed from a one-piece fuselage barrel section and hauled to Heathrow airport, where the aircraft was stored. The scorched section of the fuselage was removed and the new panel was secured in place with a bonded splice plate (a strap joint). In addition to the bonded repair the section was mechanically fastened to surrounding frames and stringers [18]. This achievement shows the extent to which adhesive bonding is used in the aircraft industry and is further reason to improve the joint design used for CFRP substrates.

2.3.2 Typical loads

When designing a bonded joint, engineers should consider maximising the bond area and try to limit localised stresses. Joints which are subjected to shear are preferred to the ones subjected to tensile loads, because an overlap length can be augmented in a more cost efficient way than the thickness of part.

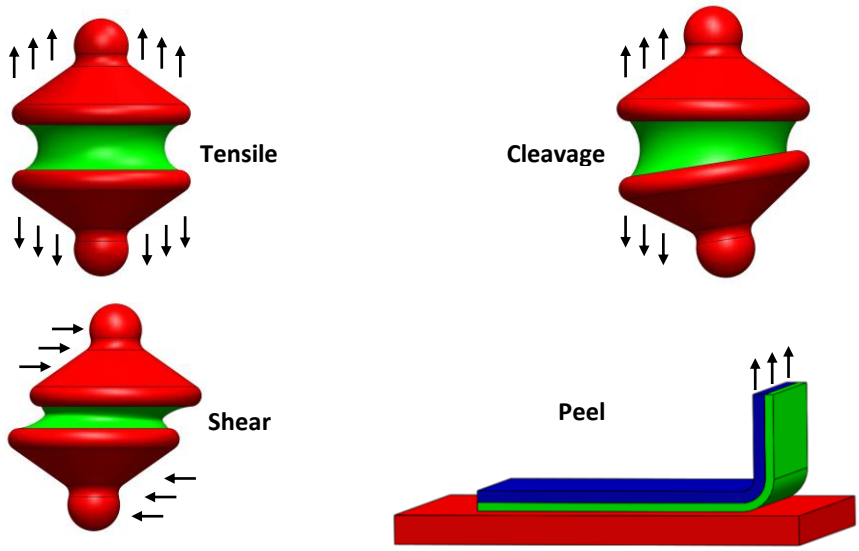

Figure 4 - Typical loads of a bonded joint

In Figure 4, the typical loads of bonded joints are presented; a tensile load is when the substrates are pulled apart on the normal direction to the bonded area. A characteristic of this type of load is that the stress is uniformly distributed across the adhesive. Cleavage is a type of load where only one end of the bonded area is subjected to stress while the other is theoretically under no stress. Adhesive joints subjected to shear loads are those bonds in which the adherends are translated across the adhesive while remaining parallel. When one of the adherends is flexible and a pulling force acts upon it the adhesive is subjected to a peel load, this type of load concentrates the stress along a thin line. In industrial applications, however, it is very hard for one to design a joint in which, only one type of stress is present, therefore a combination of loads is present.

2.3.3 Joint configuration

Bonded joints should be designed so as to minimize or to neuter, the peel stress on the adhesive. There are some typical joint configurations, which have been studied extensively, due to their simplicity and occurrence in industrial design. Figure 5 shows some typical joints that are commonly found in engineering applications.

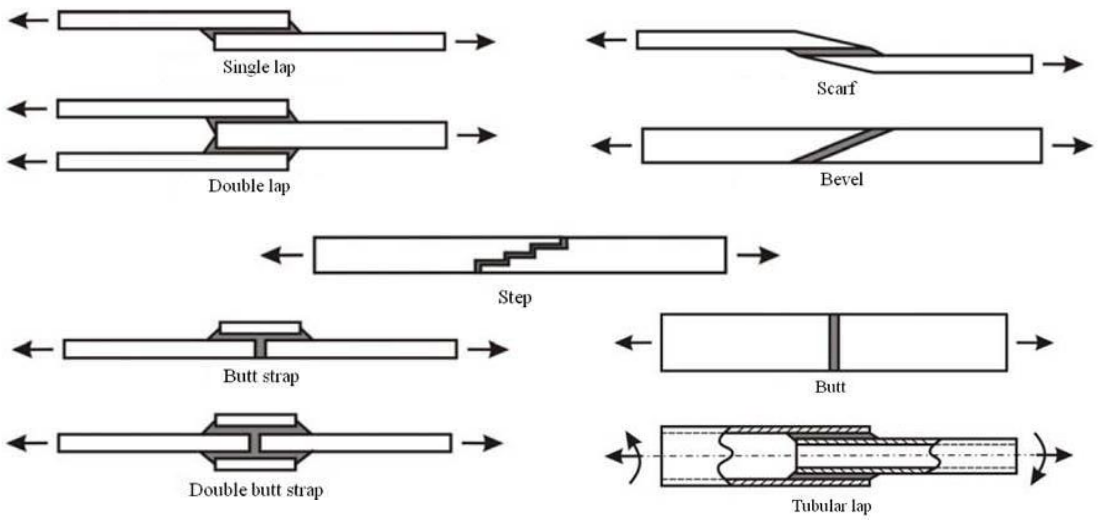

Figure 5 - Common types of bonded joints

The most used joint in industry is the SLJ, due to its simplicity and efficiency. Some variations of the SLJ have been researched due to the need of lowering the peel stress.

2.3.4 Failure modes

The failure modes of bonded joints can be classified in 3 main groups:

- Adherend failure, in one of the adherends outside the joint (Figure 6. a, b, c);
- Cohesive failure, fracture of the adhesive layer (Figure 6.d);
- Adhesive failure, between the adhesive and one of the adherends (Figure 6.e).

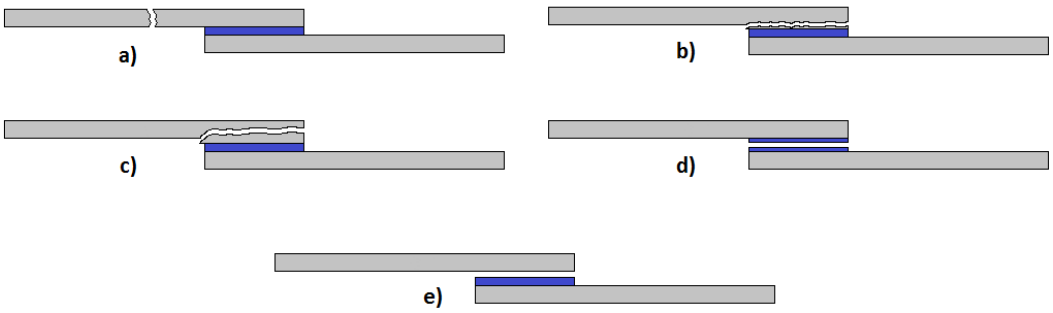

Figure 6 - Common failure modes for bonded joints

Adherend failure outside the joint, Figure 6.a, can be achieved if the adhesive bond is fabricated and designed properly. This case enables the adherends to be used to their full capabilities and is very desirable, because if the adhesive bond has a greater load capacity

than the surrounding parts, only the adherends will have to be tested to certify the structural integrity.

A particular case of adherend failure occurs when using FRP substrates. Due to peel stresses which appear in the case of lap joints and considering the poor through thickness strength of these materials, delamination of the adherends can occur (Figure 7).

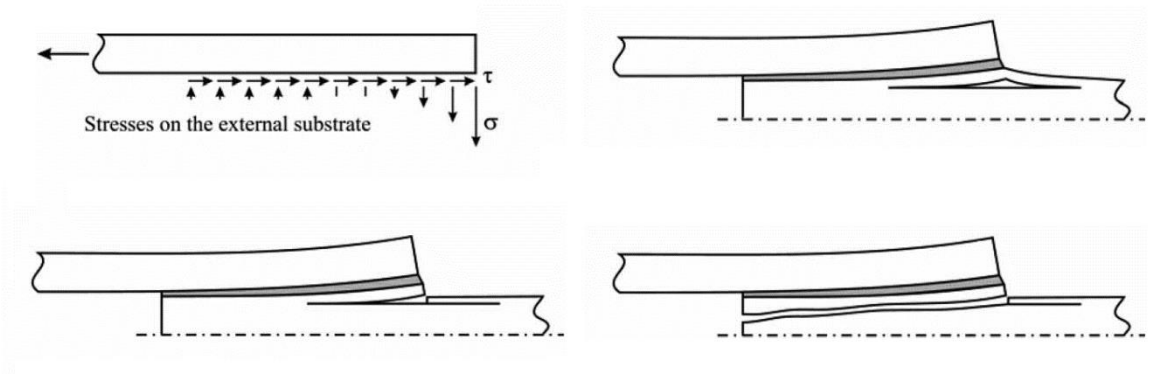

Figure 7 - Failure of the adherend joints due to transverse stresses of the composite substrates [19]

This particular case localises the failure of the adherend in the region of the bond area and can be split into two types of failure; light-fibre-tear (Figure 6.b), when some of the fibres of a lamina are pulled from the adherend and fibre-tear (Figure 6.c), when a lamina or more, are separated from the adhesive.

Due to this problem with fibre reinforced plastics, researchers proposed different solutions to lower the peel stress of the bonded joints. Different configurations of the joint have been proposed which include: adherend shaping (outside or inside tapering), adhesive fillet, using two adhesives, and so on. The objective of this thesis is to prevent these failures by improving the transverse strength of CFRPs using FMLs.

Cohesive failure, Figure 6.d, takes place when the fracture propagates through the adhesive layer and can be recognized by the presence of adhesive material on both faces of the adherend. In the case of lap joints shear loads are usually responsible for this failure, but peel stresses or a combination of shear and peel, can cause a cohesive failure. The fracture surface of this failure case can have a lighter colour tint than the bulk adhesive material [20]. In the case of film adhesives, usually, the failure occurs along the plane of the carrier cloth. This type of failure is a consequence of proper surface treatment of the adherends.

When cohesive failures occur during the service life of a product, they are typically a result of poor joint design.

Adhesive failure, Figure 6.e, can be recognized by the lack of adhesive on one of the adherends. It occurs in the plane between the substrate and the adhesive. This type of failure is a consequence of the manufacturing process.

2.4 Strength prediction of bonded joints

2.4.1 Analytical solutions

Analytical solutions for bonded joints were developed for the most common joints which are used in industry. A list of some of these solutions follows:

a) Linear elastic analysis

This analysis assumes that the adherends are rigid and the adhesive is subjected only to shear stresses. The stress value is constant across the bond area and is calculated using equation 1.

$$\tau = \frac{P}{b \cdot l} \tag{1}$$

Where P is the load, l is the overlap length and b is the joint width.

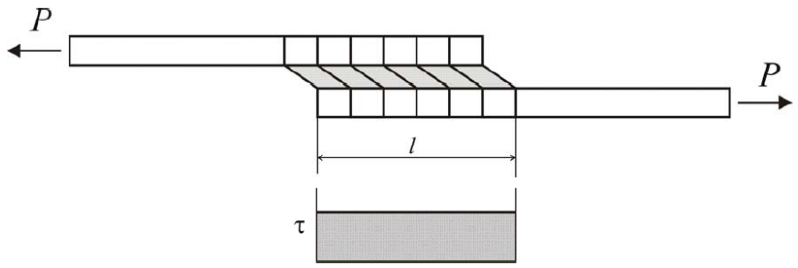

Figure 8 - Deformations and stresses in SLJ with rigid adherends [21]

b) Volkersen's analysis

Volkersen [22] developed a model where the adhesive is deformed only in shear, but the adherends are not considered rigid any more, but can be deformed in tension, as it can be observed in the Figure 9.

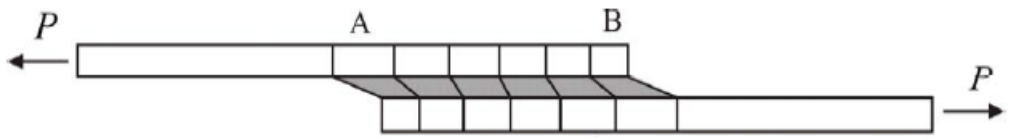

Figure 9 - Deformations of SLJ according to Volkersen [21]

The strain of the upper substrate has the maximum value in A and is zero at B. This phenomenon, combined with the continuity of the adhesive/adherend surface, leads to a non-uniform shear strain distribution in the adhesive layer. The shear stress distribution plot of such case can be observed in the Figure 10.

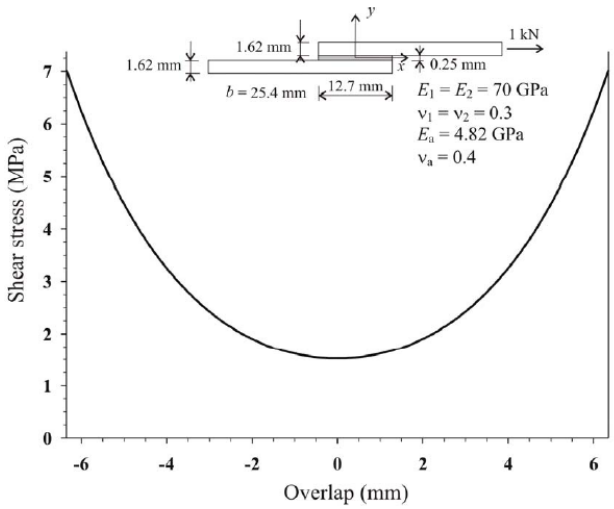

Figure 10 - Volkersen's adhesive shear stress distribution [21]

The shear stress values are maximum at the ends of the overlap and decrease towards the centre of the overlap. Unfortunately this type solution does not consider the bending effect due to the eccentric loading of the SLJ, being more suitable for the case of the double lap joint where bending of the substrates is not that significant as in SLJs.

c) Goland and Reissner's analysis

Goland and Reissner [23] were the first to consider the effects of an eccentric load path of the single-lap joint. This leads to a bending moment and a transverse force which act upon the bonded joint (Figure 11). This rotates the joint and creates a geometrical nonlinear problem, in which the large deflections of the substrates must be accounted.

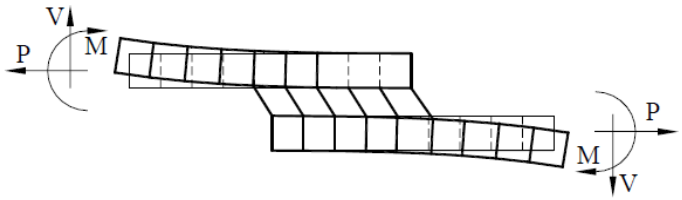

Figure 11 – Goland and Reissner's model [21]

Due to the transverse force the joint is subjected to shear and peel stresses. The shear stress distribution is similar to the one found using Volkersen's analysis, but Goland and Reissner's solution gives higher shear stress values at the ends of the joint, because the peel stresses cause additional shear stress [21].

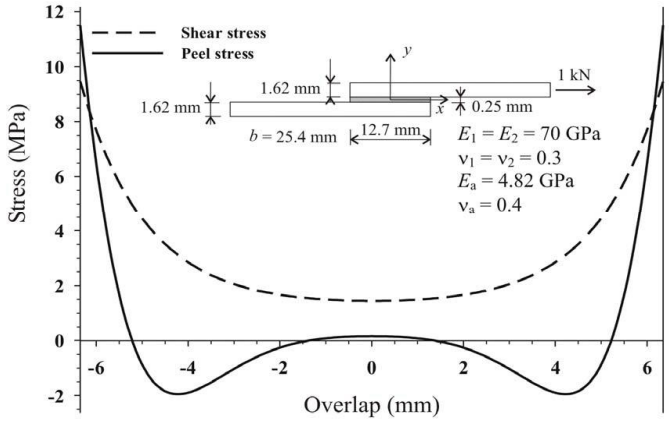

Figure 12 – Goland and Reissner's adhesive shear and peel stress distributions [21]

Volkersen, Goland and Reissner were a great leap towards failure prediction of adhesive bonds; unfortunately there are some limitations when using these analytical models. None of the above mentioned models can account for the plastic deformation of the adherends neither for the yielding of the adhesive. By ignoring the plastic deformation of the adhesives, these models are better suited for brittle adhesives than for ductile ones.

2.4.2 Continuum mechanics

The failure criterion in the continuum mechanics approach relies on the value of stress, strain or strain energy, obtained from a finite element analysis, which are then compared with the determined values for the material. The bond is assumed perfect and the constituents are modelled using continuum elements. Because of this assumption, the adhesion properties between the substrates and the adhesive are not taken in consideration.

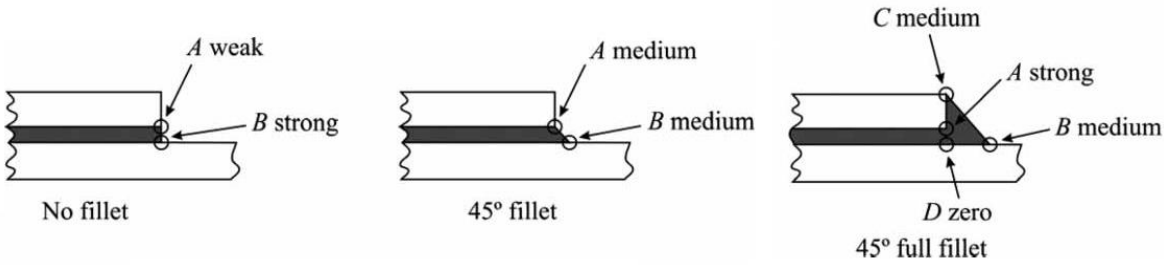

Figure 13 – Strength of singularities in adhesive lap joints [24]

Due to the singularity points at the end of a bonded joint, shown in Figure 13, it is difficult to use the maximum strain or stress criteria. Because of the fact that these singularity points will always exist at the end of a joint modelled with finite elements, the maximum strain will be found in the singularity point and the value will depend on the mesh refinement. However, in a real life case due to the manufacturing process, the corners have a rounding and are not sharp. Adams and Harris [25] have studied the influence of the rounding of corners and showed that the singularity can be removed, but the level of peak

stress became dependent on radius of the corner. This leads to the problem of knowing the exact shape, to obtain accurate predictions.

2.4.3 Fracture mechanics

When using continuum mechanics approach we have to assume that the material is continuous. This means that discontinuities or defects cannot be analysed using that approach. However cracks are usually the most prevalent defects in a bonded joint and fracture mechanics is the tool to analyse them. This approach's failure criterion is the toughness, which is an energy parameter. Values for toughness can be calculated as a function of normal and shear deformations acting at the crack tip, or the interface between adherend and adhesive or in the adhesive. Using this approach the fracture path can be predicted [26]. This approach uses linear elastic fracture mechanics which assumes the material to be linear elastic and the pre-existence of a crack.

Due to the fact that the size of a defect, in a well manufactured joint is very small and cannot be considered as a crack, and that there are materials that yield, another approach has been developed that uses fracture mechanics without initial crack, which uses a generalized stress intensity factor.

2.4.4 Cohesive zone models

In cohesive zone models fracture is considered to be a gradual phenomenon in which the separation takes place across an extended crack 'tip', or cohesive zone, and is opposed by cohesive traction [27]. That means that the cohesive zone elements (CZE) do not represent any physical material, instead they are used to represent the cohesive forces between the material layers, which develop when the material is subjected to tensile load. As a result cohesive elements are placed along a predetermined path, between continuum elements, as shown in the Figure 14.

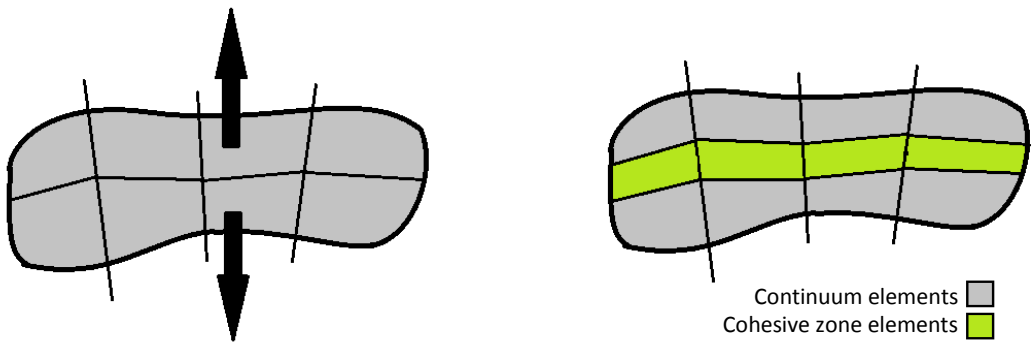

Figure 14 – Usage of cohesive zone elements along the boundary of structural elements

When the cohesive elements are subjected to a damaging load they open to simulate the crack growth or crack initiation. The crack path can follow only the CZEs, however this is not a problem when modelling adhesive bonds, because the crack usually occurs in the adhesive layer, which can be represented using a layer of CZEs.

The damage evolution is described by the traction-separation law which relates the traction forces to the separation. The first part of the traction-separation law is related to continuum mechanics, while there is no damage to the material; damage starts to occur, according to a stress based criterion and the crack propagation is described using a fracture mechanics model. Therefore, the traction-separation law represents the combination of the continuum mechanics and the fracture mechanics approaches.

There is a great variety of traction-separation laws as shown by Chandra et al. [28]; however all of them exhibit the same behaviour. When the load is applied to the model, the two cohesive surfaces start separating and traction forces appear. They increase until a maximum value is reached. If the load and traction forces are not balanced, the traction forces will decrease as the CZE is damaged according to the traction separation law. A typical traction-separation law is presented in Figure 15.

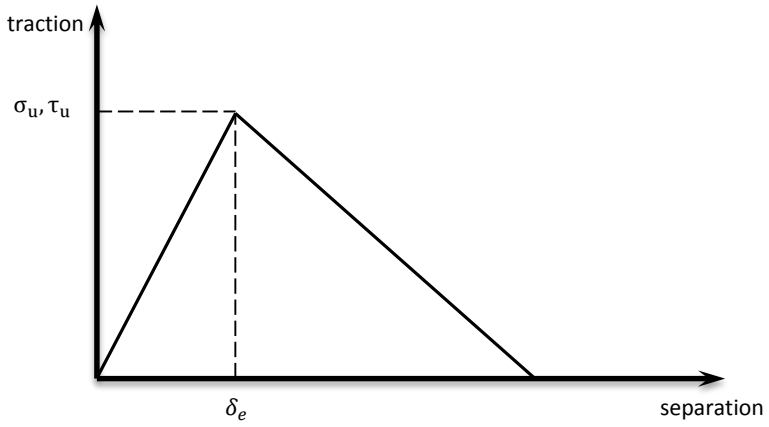

Figure 15 – Typical traction-separation response

This traction-separation law is used for tensile traction or for shear traction; the area under the curve is the fracture energy ($G_{I/IIC}$). The cohesive law implemented in ABAQUS® programme is the triangular law, which is schematically represented in Figure 15.

3 Experimental details

3.1 Adhesive

The adhesive used in this study is Araldite® AV138M1 / Hardener HV 998 supplied by HUNTSMAN. This is a two-part epoxy adhesive which is brittle and Neto, et al. [29] observed that it produces delamination on CFRP substrates if the overlap is longer than 30 mm. Due to this behaviour, this adhesive is a great tool for studying the properties regarding delamination of the joints designed during this research. The mechanical and cohesive properties of the adhesive are presented in Table 1.

Table 1 – Cohesive parameters of AV138M1/HV998 [29,30]

Parameter	Value
E [MPa]	4890
G [MPa]	1560
σ_u [MPa]	39.45
τ_u [MPa]	30.2
G_{IC} [N/mm]	0.346
G_{IIC} [N/mm]	4.91

In order to obtain the maximum mechanical properties for the joints, the mixing of the adhesive with the hardener should be in a ratio of 100:40 by weight (resin to hardener) and cured at 100 °C for 10 minutes [31].

3.2 Adherends design

This work is concentrated around improving the transverse properties of CFRP using a concept similar to the one found in fibre metal laminates. The layup was designed so as to maintain a ratio of 3:1 (by volume), CFRP to metal alloy. This ratio is a preliminary value, chosen because the object of this study is to reinforce the transverse properties of CFRPs.

The metal of choice is the 2024-T3 aluminium alloy and the primary alloying element of this material is copper. It is a high strength alloy and also has very good fatigue resistance. The 2024 alloy's main applications are aircraft structures and parts for the transportation industry. This aluminium alloy is used extensively to manufacture FMLs, as five out of six GLARE grades and two out of four ARALL laminates have 2024-T3 in their structure [7]. It is known that between CFRP and aluminium, galvanic corrosion appears due to the difference of electrode potential, however, studies are conducted which have the aim of finding a surface treatment which provides good protection against this

phenomenon [9]. Another metal alloy that can be used, is the Titanium alloy Ti-6Al-4V (more commonly known as Grade V), which does not exhibit galvanic corrosion, has higher strength values and lower linear thermal expansion coefficient. Unfortunately during the period of this study it could not be found at any of the traditional suppliers.

The 2024-T3 alloy was supplied in sheets with the dimensions of 300 mm x 300 mm x 0.8 mm and the mechanical properties are presented in Table 2.

Table 2 – Mechanical properties of 2024-T3 aluminium [32]

Parameter	Value
E [MPa]	73100
G [MPa]	28000
σ_y [MPa]	289
σ_u [MPa]	434 - 441
ε_u [%]	10 - 15

Because sheets of aluminium with a thickness of 0.4 mm were not in stock with the traditional suppliers, only sheets with the thickness of 0.8 mm were used. Considering the ratio of 3:1 by volume, CFRP to Al, this leads to minimum thickness of the laminate of 3.2 mm, if only one sheet of metal is introduced. In order to evaluate different stacking orders for the laminate, configurations with two sheets of aluminium will also be manufactured. In the case of laminates which have two sheets of aluminium introduced, the thickness of the adherend will be 6.4 mm according to the assumed ratio. The bonding between the aluminium and the CFRP will be realised in the hot plates press during the cure of the CFRP.

Due to the unavailability of studies regarding this type of laminates, the selected stacking orders were chosen to be representative of different configurations and to ease the manufacturing process. The layups which will be manufactured and tested are presented in Figure 16.

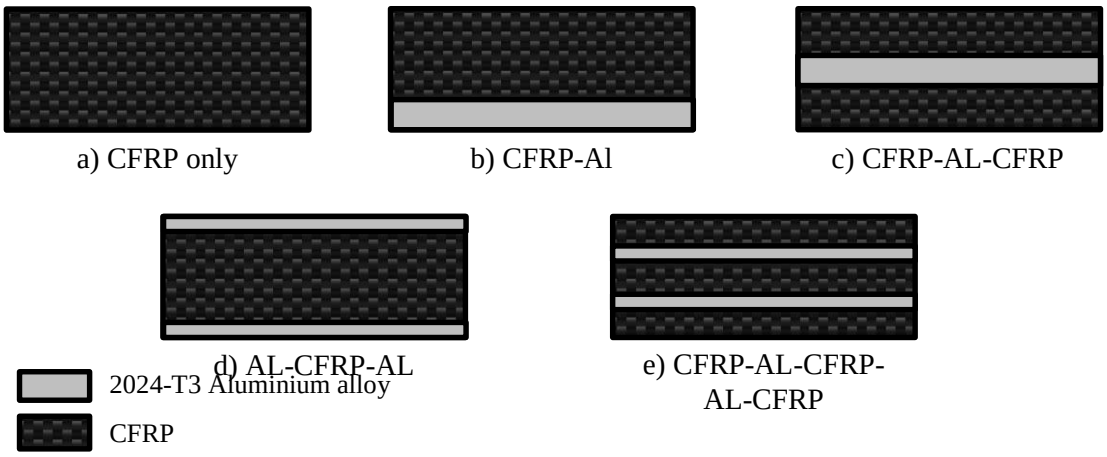

Figure 16 – Selected layups

The adhesion between CFRP and the aluminium alloy will also be studied. For that purpose specimens with different surface treatment were manufactured. The surface treatments that were analysed are:

- As supplied;
- Sandblasted;
- Phosphoric acid anodizing.

3.3 Specimen manufacture

3.3.1 Manufacture of the CFRP plates

The manufacture of the CFRP plates was performed using a unidirectional (0^o) prepreg, with the layer thickness of 0.15 mm, using hand lay-up method and cured in a hot plates press. The manufacturing process involves the following steps:

1. Thawing the prepreg (which was stored in the freezer).
2. Cutting the prepreg in squares of 300 mm x 300 mm.
3. Stacking the laminate by hand lay-up (respecting the predefined sequence). During this step the layers are stacked one at a time, after removing the Teflon coating and subsequently are heated (Figure 17.a) to ease the adhesion between the plies. This is followed by the application of pressure on the entire surface with a scraper (Figure 17.b) and removal of the paper coating.

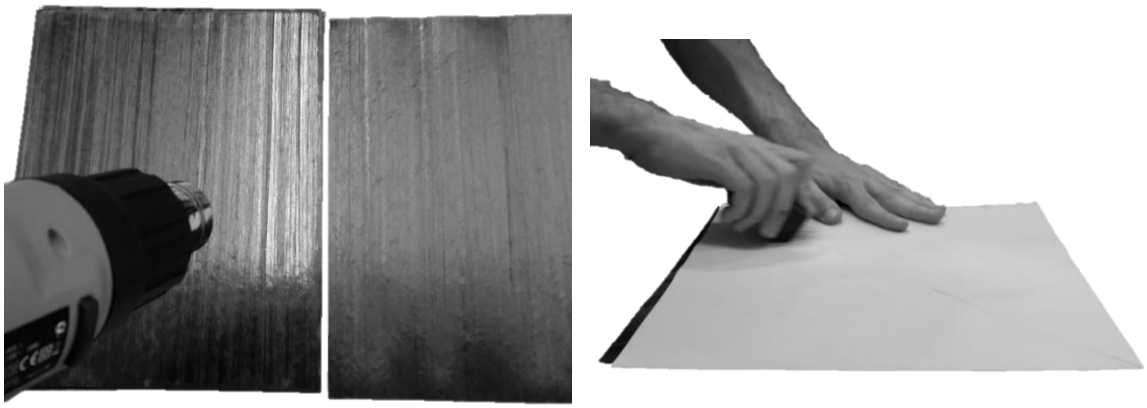

a) b)

Figure 17 – Laminate manufacture, heating of the layers (a), applying pressure on the surface (b)

4. After the manual lay-up of all the layers, the laminate is placed in the mould (Figure 18). Spacers were selected to ensure the correct thickness of the composite. To facilitate the removal of the laminate from the mould, three coats of a releasing agent (Loctite® Frekote 770-NC™) were applied to it and to the spacers.
5. The mould is placed in a hot plates press (Figure 19.a) and cured according to the cycle recommended by the material supplier (Figure 19.b). The cycle consists of gradual heating with a slope of 4°C/min, maintaining the composite at a temperature of 130°C for one hour under a pressure of 4 bar and gradually cooling down the composite with the same slope used for heating.

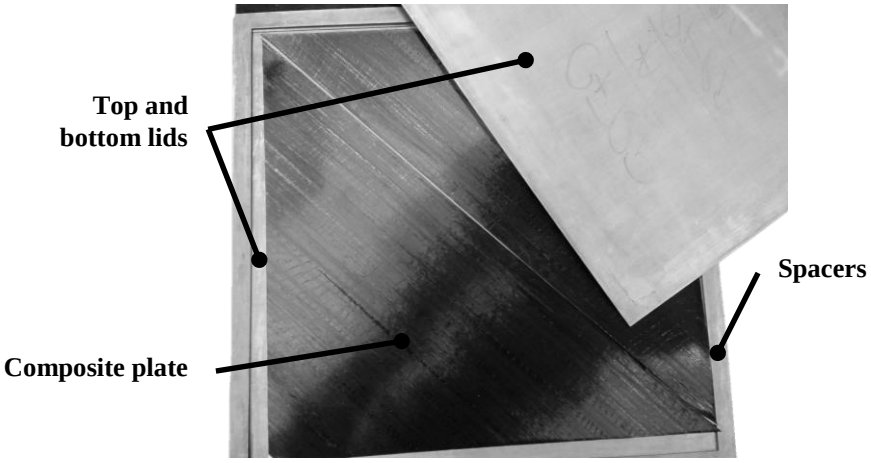

Figure 18 – Mould used to cure the composite

6. After curing, the composite plates are cut to specimen size using a circular saw equipped with a diamond coated disc.

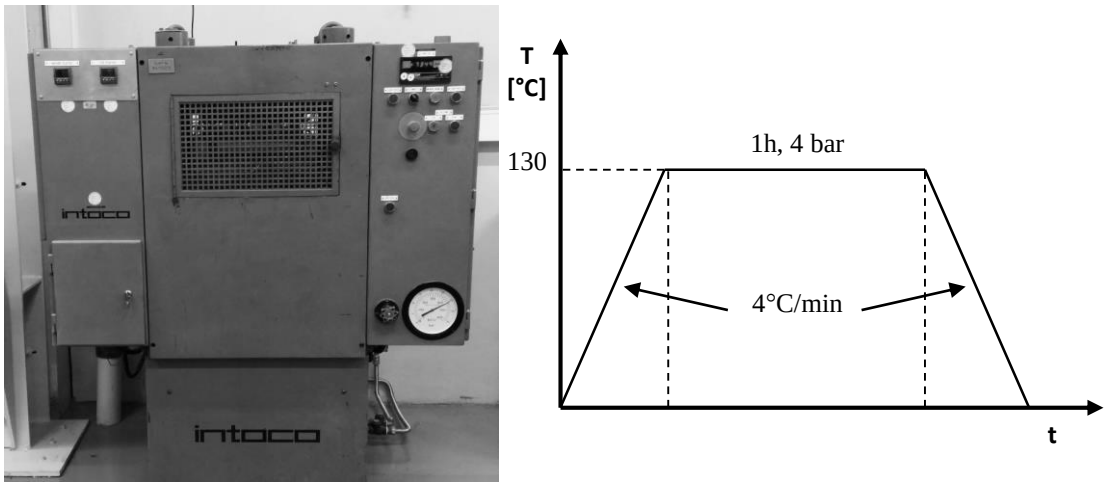

Figure 19 – Curing of the composite plates, the hot plates press (a) and the curing cycle (b)

3.3.2 Manufacture of the CFRP-Aluminium laminate

The manufacturing of the laminate follows the steps described in 3.3.1 to which the step of laying up the aluminium sheets was added. This step is represented in Figure 20.

Figure 20 – Laying up the aluminium sheets, one by one

To facilitate the bonding between the aluminium and the CFRP; after laying up they were heated using a hot air gun and pressed firmly on the layers of CFRP.

3.3.3 Surface treatment of the aluminium alloy

In order to evaluate the bond properties between the epoxy resin used in the CFRP prepreg and the aluminium sheet three surface treatments were used. The surface treatments will be explained in this section of the thesis.

a) As supplied

As supplied state means that no surface treatment is applied to the aluminium. The only pre-bonding process applied is degreasing the surface using acetone.

b) Sandblasting

Sandblasting or abrasive blasting is a process of forcibly propelling a stream of abrasive material against a surface, under high pressure, to roughen a smooth surface, to smooth a rough surface or to remove surface contaminants. In this case, sandblasting is used to create a rougher surface, in order to improve the bond between the CFRP and aluminium. The process was realised using a sandblasting machine produced by de Laurentiis, model 705 GM, maintaining a distance of at least 40 cm between the nozzle and the sheet, in order to prevent the bending of the aluminium.

After sandblasting the sheet was degreased and the remaining contaminants were removed, using acetone. The cleaning process was employed just before the manufacture of the laminate, in order to assure the least contaminated surface possible.

c) Phosphoric acid anodising

The process of phosphoric acid anodizing (PAA) as a pre-treatment for adhesive bonding of aluminium alloys was patented by Marceau et al. [33] and is the precursor of the BAC 5555 standard [34].

Anodising is an electrolytic passivation process through which the natural oxide layer on the surface of a metal part is artificially increased in order to reduce the effects caused by environmental factors such as air and water, increasing the resistance to corrosion and wear, and also providing better adhesion.

The oxide layer is grown by passing a direct current through an electrolytic solution. The part that has to be anodised is used as the anode in the setup (Figure 21). Passing current through the electrolyte releases hydrogen at the cathode and oxygen at the surface of the aluminium anode, resulting in a layer of aluminium oxide.

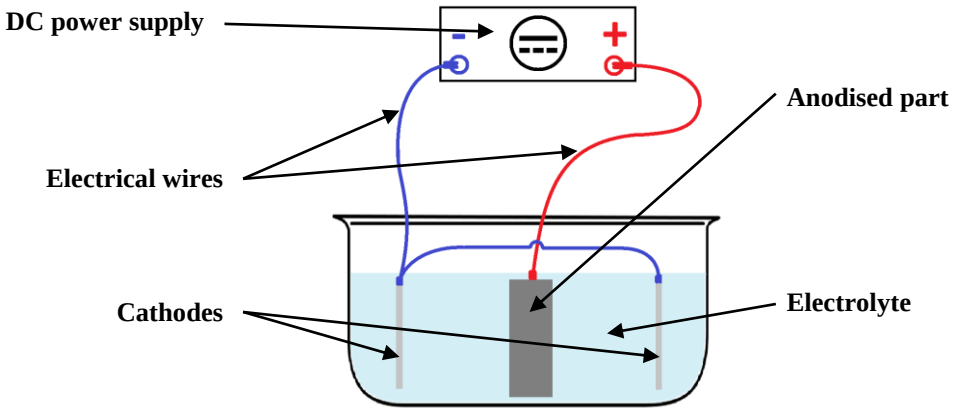

Figure 21 - Schematic representation of the anodisation process

The standard consulted and used for the anodising process, was ASTM D 3933–98 [35]. The parameters used to treat the surface of the aluminium are presented in the Table 3.

Table 3 – Parameters used for PAA surface treatment

Parameter	Value
Phosphoric acid	12 wt%
DC Voltage	15 - 16 V
Time	25 min

The anodising process employed is composed of the following steps:

1. Manually abrasion of the surface using a 800 grit sandpaper, until the outer layers are completely removed;
2. Cleaning and degreasing the surface, using a lint free cloth and acetone;

3. Introducing the sheet in the electrolyte bath, turning on the power supply and waiting for 25 minutes (Figure 22);
4. Turning off the power, removing the sheet from the electrolyte bath and rinse it under a stream of cold water;
5. To eliminate the remaining water on the aluminium sheet, a cold air blower was used;
6. To assess the quality of the oxide layer, a visual inspection was carried out;
7. The anodised part was then loosely packed into aluminium foil to protect the surface from contaminants.

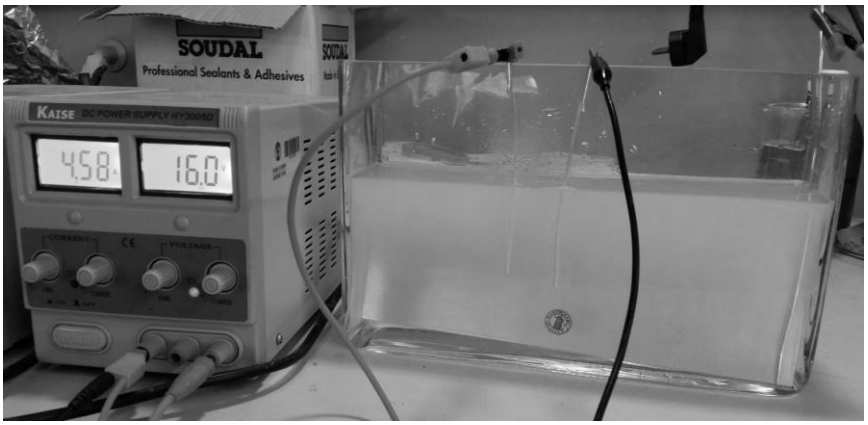

Figure 22 - Setup used for PAA

To minimize the consumption and post-processing of the phosphoric acid electrolyte, the decision of cutting the 300 mm x 300 mm sheet into smaller sheets, with the dimensions of 300 mm x 100 mm, was taken.

3.3.4 Manufacture of the single-lap joints

The main objective of this thesis is to assess the possibility of improving the transverse strength of carbon fibre reinforced plastics. To accomplish this objective, single lap joints with an overlap of 12.5 mm and 50 mm were manufactured. The overlap lengths were established after analysing the data obtained by Neto, et al. [29]. In the case of 50 mm overlap length, delamination of the adherend is expected, while in the other case the failure of the adhesive is the main goal.

The geometry of the joints is detailed in Figure 23. The width of the joint is the same for both types of joint configuration, and equal with 25 mm.

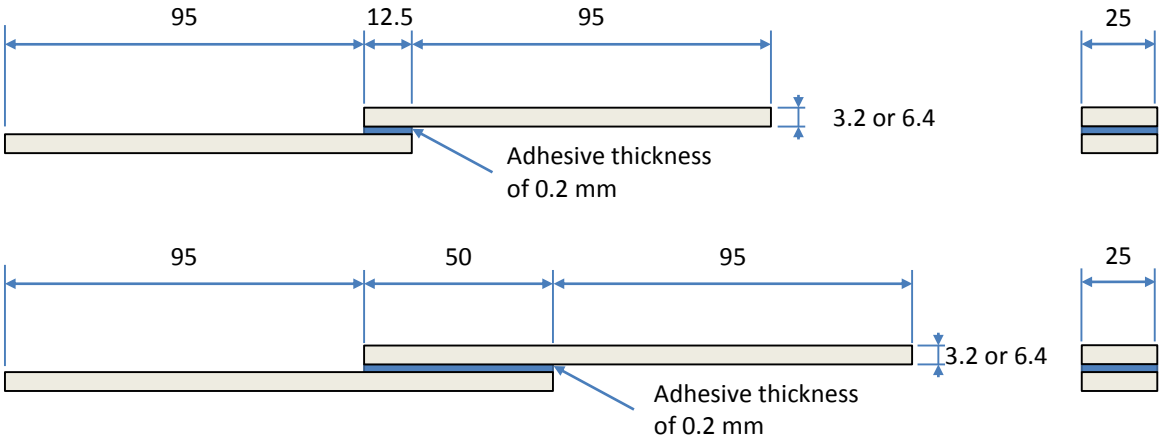

Figure 23 - Geometry of the single lap joints (all dimensions are in mm)

After the cutting of the substrates to the specific size (either 107.5 mm or 145 mm), the overlap surface is abrased using a 160 grit sand paper, forming a X pattern, until a matte surface is obtained. Cleaning of the specimen is ensured using a lint-free cloth and acetone. The wiping of the specimen is repeated, changing the part of the cloth that is used, until there are no traces of carbon residues on the cloth.

Before using the mould, it must be coated with releasing agent to ensure easy removal of the specimens after the curing ends. Spacers were used to maintain the correct thickness of the adhesive layer (Figure 24).

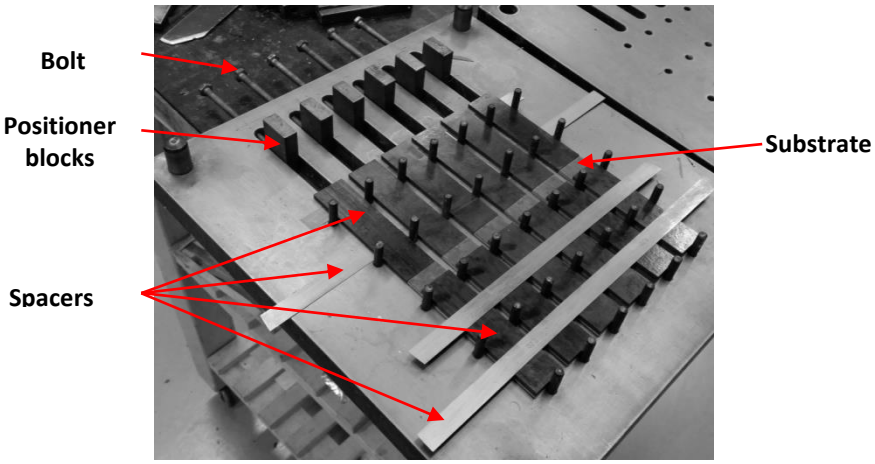

Figure 24 – Mould used to manufacture the joints; prepared for the application of adhesive

Figure 25 – Application of the adhesive

After the application of the adhesive (Figure 25), the mould is closed and placed in the hot plates press for one hour at 100°C using a force of 1200 kgf. With the curing of the adhesive complete, the excess adhesive is removed using a file and 160 grit sand paper. To ensure that the loading axis of the testing machine is collinear with the adhesive, 25 mm x 25 mm tabs, with the thickness of the substrate, are bonded at each end of the joint.

3.4 Surface treatment influence

The influence of the surface treatment was a point of this study. In order to evaluate the bond quality between aluminium and CFRP, three plates were manufactured (with the lay-up as depicted in Figure 16.c). Each plate had one of the surface treatments presented in 3.3.3.

While cutting the plates, the one which had aluminium as supplied exhibited the worst adhesion. The CFRP debonded (Figure 26) on both sides of the aluminium, only due to the thermal stresses induced in the aluminium.

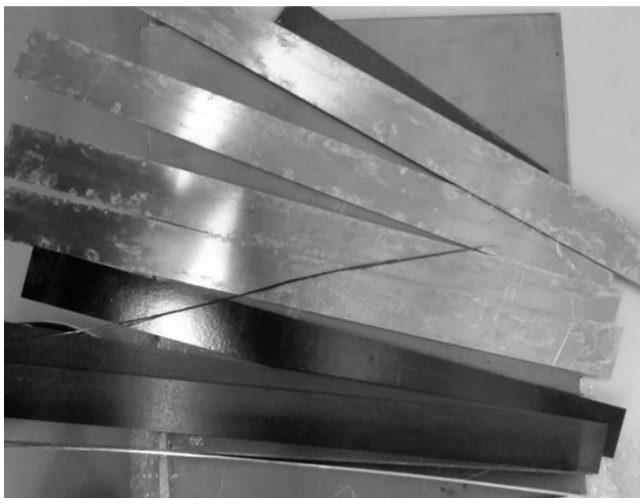

Figure 26 - Debonding of the CFRP from the aluminium

The plates on which sand blasted aluminium was used exhibited better adhesion properties, but debonding occurred while cutting (Figure 27.a) in around 75% of the cases while the rest debonded after a week (Figure 27.b), due to residual thermal stresses.

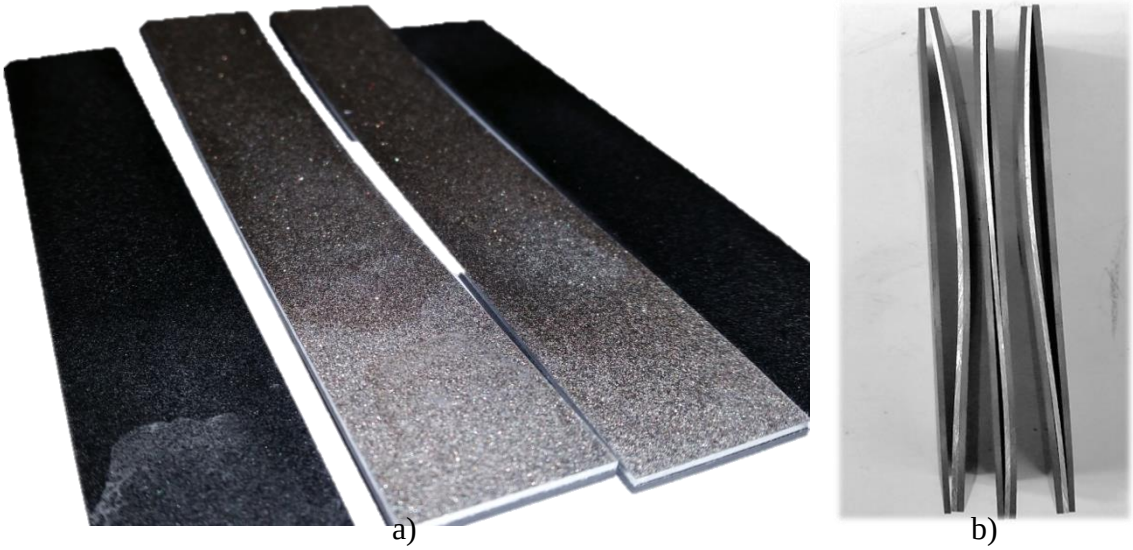

a) b)

Figure 27 – Debonding of the CFRP with sandblasted aluminium; a) debonding occurred while cutting, b) debonding occurred after a week

The plate where a PAA surface treatment has been used exhibited very good adhesion properties compared to the other treatments. The adhesion was tested using three methods: traction test in mode I, three point bending and a peel test with pre-crack. The results of these tests are presented in the following sections.

Table 4 – Comparison between surface treatments

Surface treatment	Results
As supplied	Delaminated while cutting
Sand blasted	Delaminated while cutting
Phosphoric acid anodisation	Exhibits good adhesion

3.4.1 Traction test in mode I

To evaluate the adhesion properties between the anodised aluminium sheet and the CFRP, a traction test in mode I was used. To load in mode I, two steel blocks were bonded to a specimen (Figure 28.a). Every steel block has a hole with the diameter of 5 mm, through which a steel pin is introduced, which also connects the specimen with the testing

machine's grips. The loading setup is presented in Figure 28.b. Three specimens were manufactured to be tested.

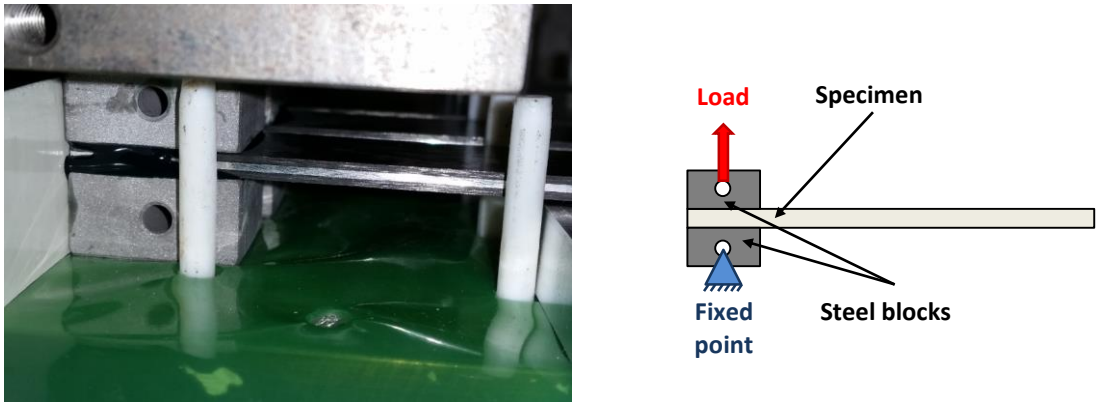

a) b)

Figure 28 – Traction test in mode I; a) specimen used, b) loading scheme

The failure of the laminate was situated in the CFRP layer, just above the aluminium sheet (Figure 30). The average failure load was 14.52 ± 1.37 kN; a representative P-δ curve is presented in Figure 29.

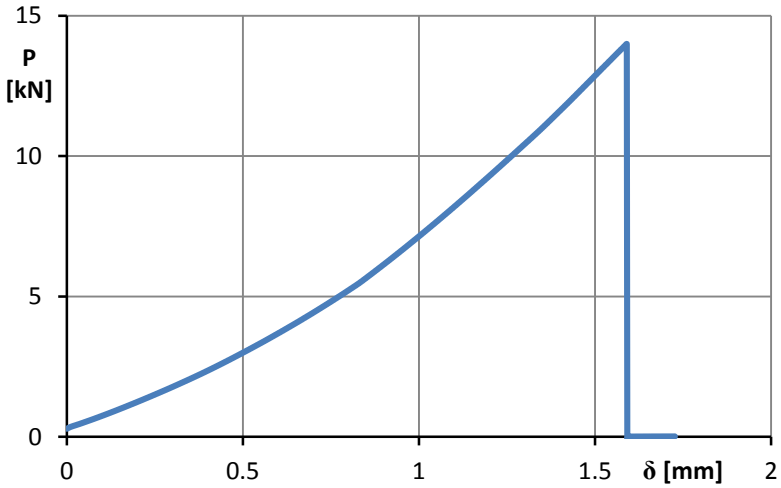

Figure 29 - Most representative curve for Mode I traction test

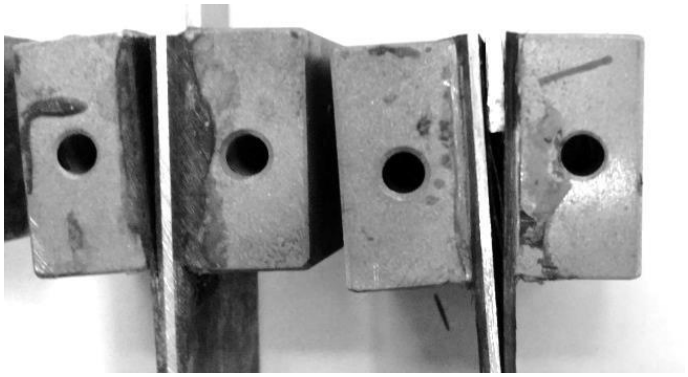

Figure 30 - Typical failure of the laminate in mode I traction test

3.4.2 Three point bending

Cohesive properties should be characterized in traction and shear. Because the laminate exhibited good adhesion properties, in mode I, between aluminium and CFRP, additional tests were conducted to evaluate the adhesion properties in mode II. In order to accomplish this, a three point bending test was employed.

The specimens were tested according to standard ASTM D790 [36], in an INSTRON® model 3367 universal test machine with a capacity of 30 kN, at room temperature and constant displacement rate of 1 mm/min. Preliminary tests were realized to identify the best setup of the test rig. The span between the supports was fixed at 100 mm but different configurations for the load roller were accounted. In order to limit the contact pressure four possible setups were tested; the configurations and the results are presented in Table 5. The four setups considered are:

- 30 mm roller;
- 30 mm roller with a piece of silicone between the specimen and the roller;
- 60 mm roller;
- 60 mm roller with a piece of silicone between the specimen and the roller.

The tests were conducted on specimens manufactured only with CFRP and the silicone was considered as a mean to lower the contact pressure. Two specimens were tested for each of the setups considered.

Table 5 - Configurations for the loading roller and results

Configuration	Maximum load [kN]
Ø30	2.35
Ø30 with silicone	3.23
Ø60	3.45
Ø60 with silicone	3.76

The results of the tests indicated that the best configuration to be used is the one with the loading roller with a diameter of 60 mm and a piece of silicone rubber between the roller and the specimen. The type of failure obtained using this setup was fibre failure in the whole thickness, while the specimens tested using the smaller roller exhibited a failure typical for contact pressure, with matrix and fibre breaking only in the vicinity of the loading point. The testing rig is represented in Figure 31.

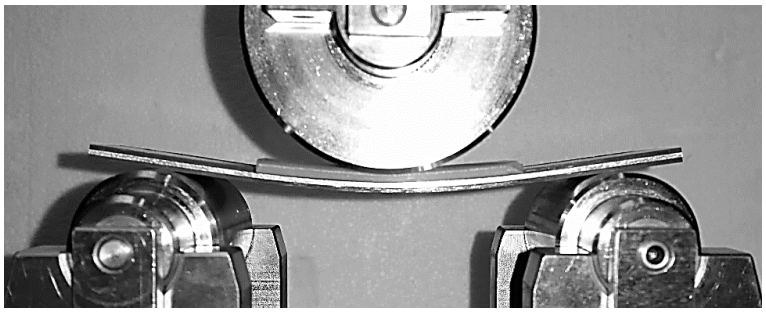

Figure 31 - Test rig used for the three point bending test

In order to evaluate the strength of the laminate four specimens were tested. Because the comparison between the laminate and the reference (only CFRP) is important, four specimens of the reference geometry were also tested. The most represantative P-δ curves are represented in the Figure 32.

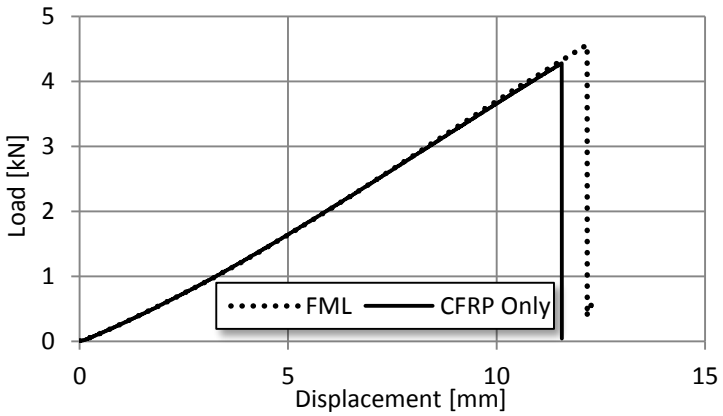

Figure 32 – P-δ curves for the three point bending test

The failure of the laminate was characterized by fibre failure in the upper region of the specimen, this is due to compression stresses induced by the thermal contraction of the aluminium, while in the case of the reference specimen the failure mode was a generalized fibre breakage though the thickness of the CFRP. The average results were: 4.54 ± 0.098 kN for the approach similar to a FML and 4.23 ± 0.434 kN for the reference specimen composed of only CFRP. The load bearing capabilities of the laminate are slightly higher than the ones of the reference joint. The adhesion between the CFRP and aluminium is very good and no delamination could be observed at the interface.

3.4.3 Peel test with pre-crack

The bond between the anodised aluminium and CFRP exhibited very good properties. In order to try to evaluate the cohesive properties between these substrates, three specimens with an artificial pre-crack were manufactured. The length of the pre-crack was set to 55 mm, and to obtain it, the aluminium plate was coated with three coats of releasing agent and a Teflon film was laid between the aluminium and the CFRP.

Loading of the specimen (Figure 33) was employed in the same way depicted in Figure 28.b; the loading was controlled using a displacement rate of 2 mm/min.

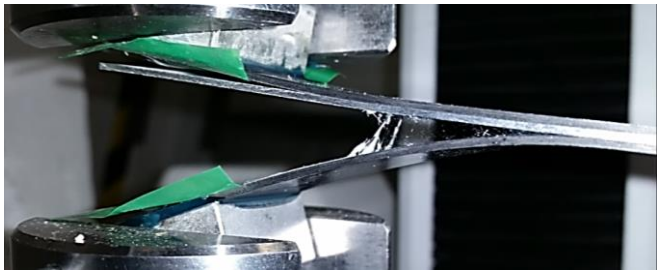

Figure 33 – Peel testing with pre-crack

In Figure 33 the tearing of the fibres can be observed, this is a sign of very good adhesion between the CFRP and aluminium. After controlled opening of the specimen for 40 mm, the displacement of the testing machine was manually controlled in order to separate the specimen and to observe the failure surface (Figure 34).

Figure 34 – Failure surface of the peel specimen with pre-crack

The surface depicted in Figure 34 shows that the adhesion between the carbon fibre and the aluminium surface which has been treated using PAA, is stronger than the adhesion between the layers of carbon fibre. Due to these results, the test could not be used to determine the mode I fracture energy for the cohesive properties of the interface. A representative P- δ curve is presented in Figure 35.

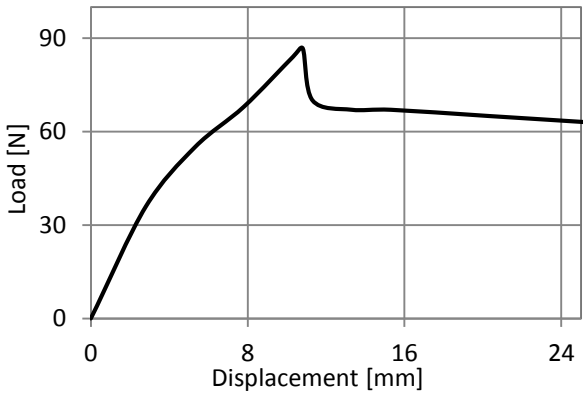

Figure 35 – Most representative curve for the peel test with pre-crack

These results indicate that, for the surface treatment of the aluminium, PAA is the best solution among the ones studied in this research.

4 Experimental results

4.1 Results of the single lap joint, test with 12.5 mm overlap

In order to test the behaviour of the composite, three specimens were manufactured for each lay-up configuration, except the one depicted in Figure 16.b. That lay-up was discarded because of the elastic instability phenomenon, mainly due to compression loads in the composite and caused by high residual thermal stresses. This problem will be assessed in the numerical work chapter of this thesis (5.1).

The specimens were tested according to standard ASTM D1002-01, using an INSTRON® model 3367 universal test machine with a capacity of 30 kN, at room temperature and constant displacement rate of 1 mm/min. To fix the specimens, two mechanical wedge-action grips (Figure 36.b) were used.

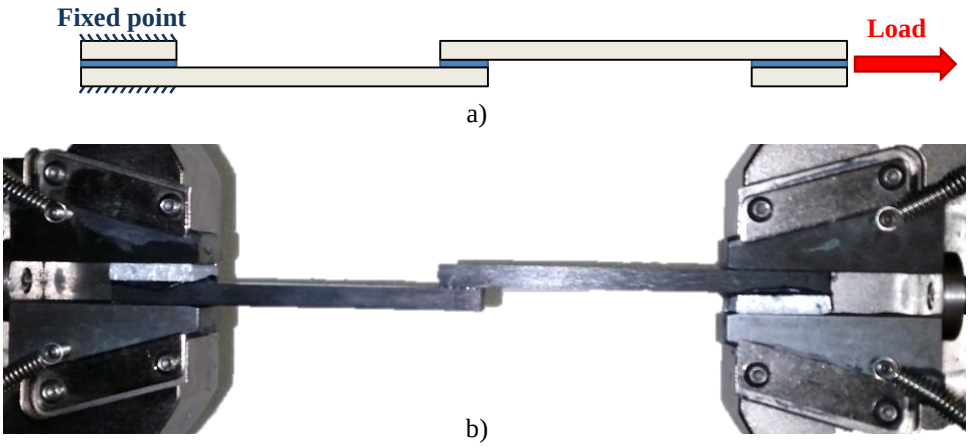

Figure 36 – Loading of the single lap joints; a) schematic SLJ test b) loading set-up

4.1.1 CFRP-only, reference joints

In order to assess the improvement obtained by creating a laminate with metal layers, reference joints were manufactured with substrates made out of CFRP only. Because there are two different laminate thicknesses, two sets of reference joints were manufactured.

The P-δ curves obtained are presented in the Figure 37. The difference in the slope of the curves was found to be caused by the slippage of the grips on the specimen, resulting in larger displacement outputs recorded by the testing machine compared to the real displacement of the joint.

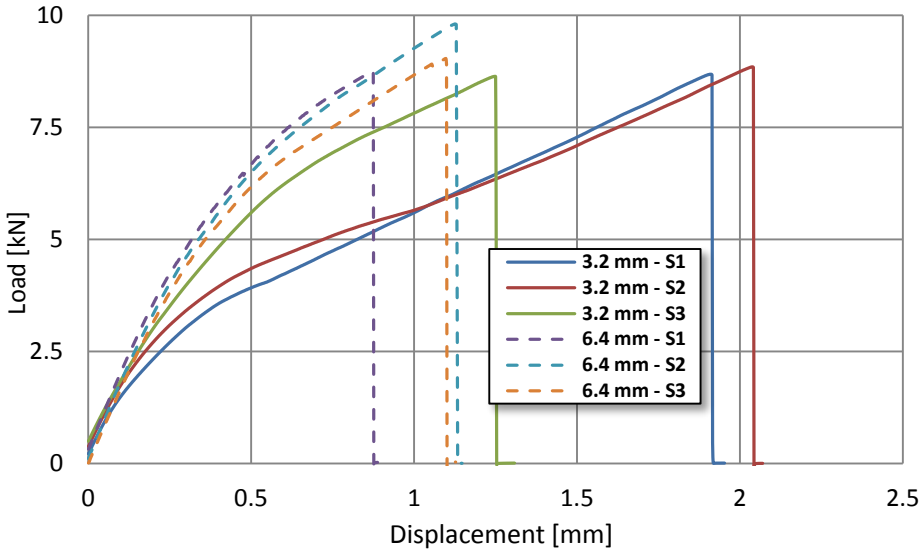

Figure 37 – P-δ curves obtained for reference joints with an overlap of 12.5 mm

The failure (Figure 38) was cohesive for both configurations and a slight increase in the maximum load was observed, with the increase of the thickness of the laminate.

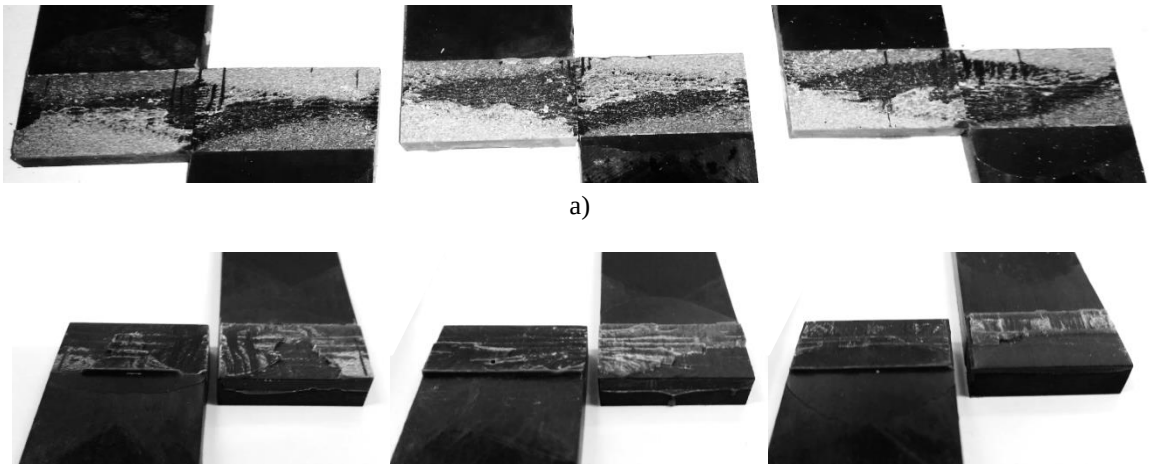

a)

b)

Figure 38 – Failure surface of the reference single lap joints: a) adherend thickness of 3.2 mm; b) adherend thickness of 6.4 mm;

The joints manufactured using the thicker adherend have a higher maximum load compared to the normal adherend. This can be attributed to the higher longitudinal stiffness of the thicker specimen, which reduces the bending of the specimen, decreasing the peel stresses in the adhesive [23]. The failure surface of the joints depicted in Figure 38.a, is a typical cohesive failure, initiated by peel stresses at the end of the overlap, while in the case of the thick adherends the failure mode is cohesive near the interface and the failure surface is typical for brittle adhesives. The average results are presented in Table 6.

Table 6 – Average failure loads and stresses for the reference geometries

Specimen thickness	Average load [kN]	τ [MPa]
3.2 mm	8.72±0.11	27.9±0.35
6.4 mm	9.196±0.55	29.4±1.76

Comparing the joints lap shear stresses to the absolute strength values of the adhesive, presented in Table 1, it can be observed that the values are very similar. This means that the adhesive is working to the maximum of its capabilities, which is expected for the small overlap studied.

4.1.2 CFRP-AL-CFRP – type laminate

This laminate exhibited very good properties when tested in three point flexural bending (3.4.2), increasing the maximum load by 7.3% comparing with the reference manufactured of only CFRP. The failure mode of this joint was also cohesive (Figure 39); the lighter areas being the result of the peel stresses to which the adhesive was subjected. The maximum load values are a bit lower compared to the reference geometry with the thickness of 3.2 mm.

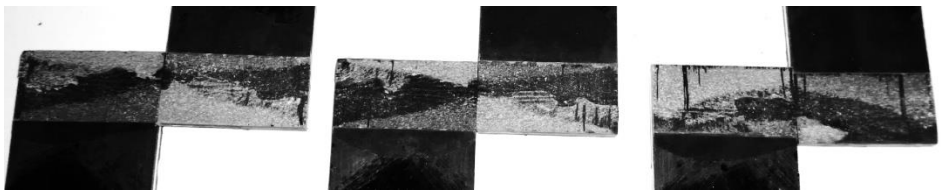

Figure 39 – Failure surface of the single lap joints using CFRP-AL-CFRP-Type laminate, 12.5 mm overlap, 3.2 mm adherend thickness

The average failure load of this joint was 8.40 ± 0.21 kN which is a bit lower that the reference geometry and corresponds to lap shear strength of 26.9 ± 0.67 MPa. The P-δ curves obtained are depicted in the Figure 40.

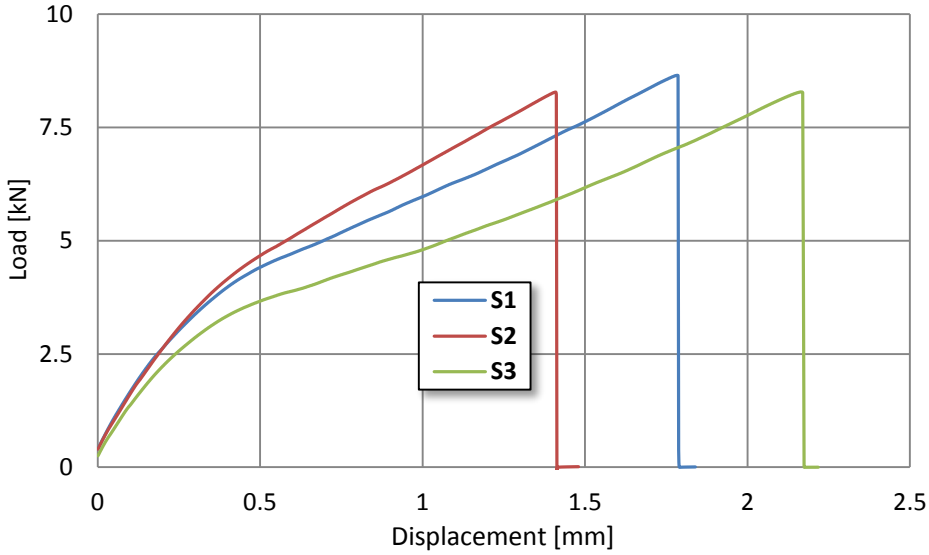

Figure 40 – P-δ curves obtained for CFRP-AL-CFRP-Type joints with 3.2 mm adherend thickness and an overlap of 12.5 mm

As with the previous tests the difference in slope between the curves, is due to slippage of the grips on the specimens. If we are to compare the reference joint with this one, the maximum load decreases by 3.67%.

4.1.3 CFRP-AL-CFRP-AL-CFRP – Type laminate

This layup is depicted in Figure 16.e and is an alternative design of the CFRP-AL-CFRP-Type laminate. The failure of this joint was cohesive near the interface and is depicted in Figure 41.

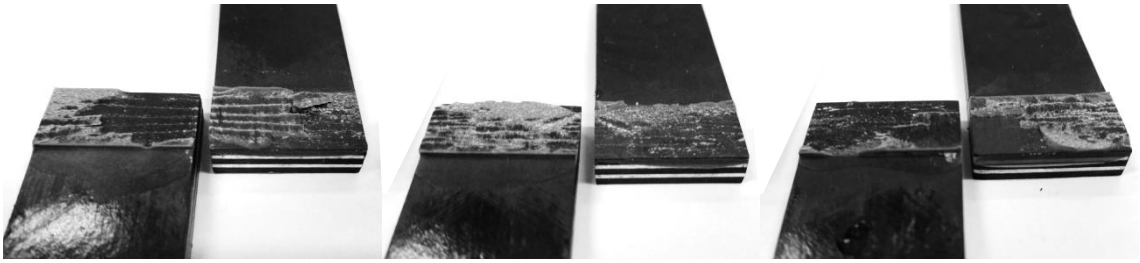

Figure 41 – Failure surface of the single lap joints using CFRP-AL-CFRP-AL-CFRP-Type laminate (6.4 mm thickness)

The average failure load for this joint was 8.40 ± 0.83 kN which corresponds to a lap shear strength of 26.9 ± 2.65 MPa, which represents a reduction of 7.69% over the reference joint. The P-δ curves obtained are depicted in Figure 42.

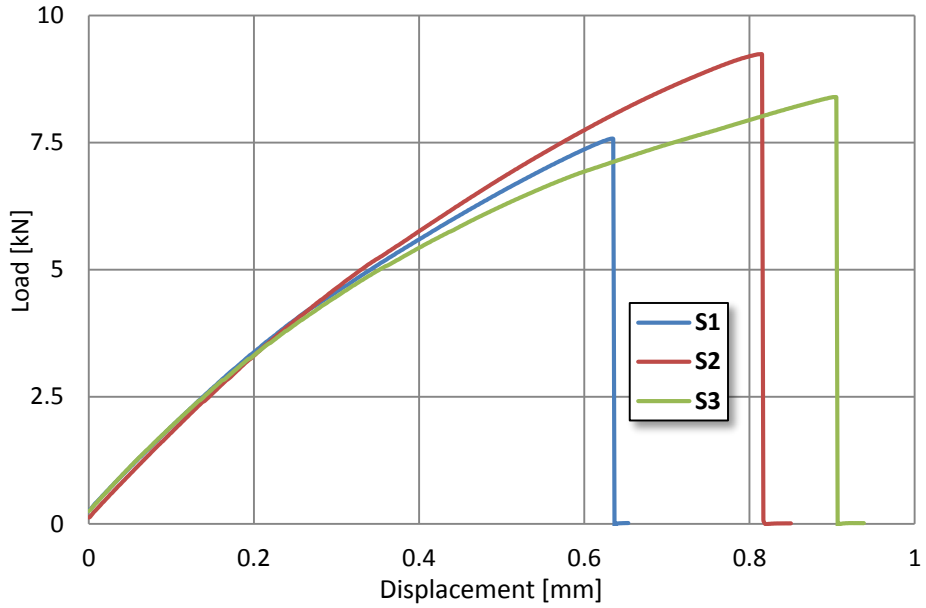

Figure 42 – P-δ curves obtained for CFRP-AL-CFRP-AL-CFRP-Type joints with an overlap of 12.5 mm and 6.4 mm adherend thickness

4.1.4 AL-CFRP-AL – Type laminate

The lay-up of this laminate is an adaptation of the classic fibre metal laminate being a sandwich of carbon fibre between aluminium sheets. Considering all the joints with 12.5 mm overlap which were studied, this lay-up exhibited the best properties of all. The failure of the adhesive was cohesive and is depicted in Figure 43. The crack front propagates through the adhesive, near the interface, jumping to the other interface at one moment.

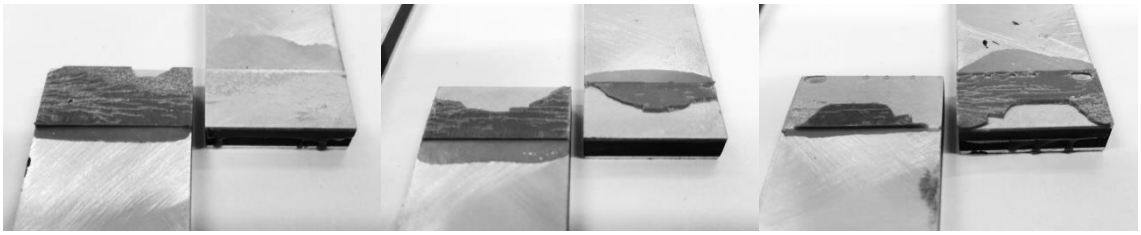

Figure 43 – Failure surface of the single lap joints using AL-CFRP-AL-Type laminate (6.4 mm adherend thickness)

The average failure load was equal to 9.6 ± 0.155 kN which corresponds to 30.72 ± 0.5 MPa a value slightly higher than the one presented in Table 1. The P-δ curves obtained during testing are presented in Figure 44.

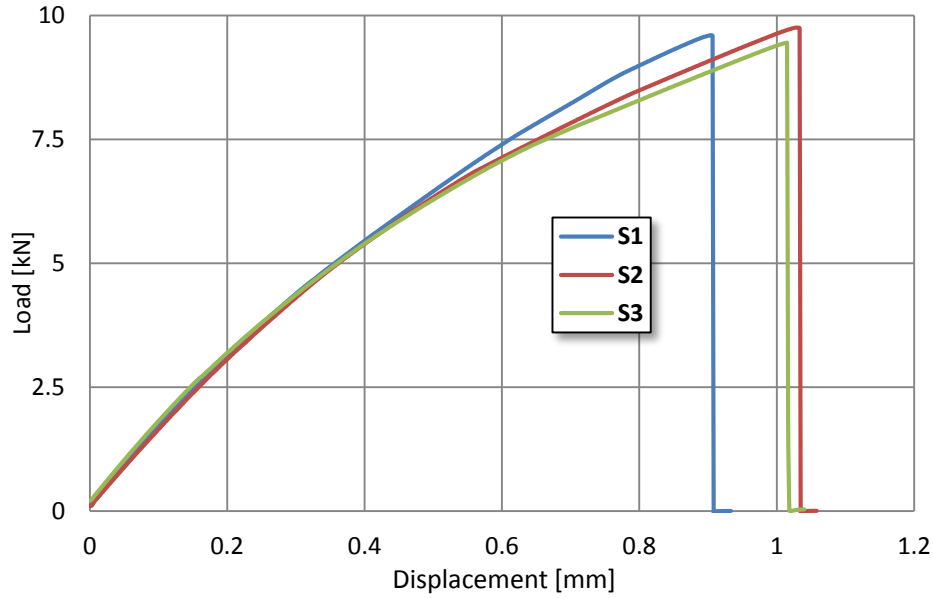

Figure 44 – P-δ curves obtained for AL-CFRP-AL-Type joints with an overlap of 12.5 mm and 6.4 mm adherend thickness

Among all the layups tested for the 12.5 mm overlap, this one has the highest average failure load.

4.2 Results of the single lap joint, test with 50 mm overlap

In order to evaluate the behaviour of the composite regarding delamination, joints with a 50 mm overlap were manufactured. According to the study realised by Neto, et al. [29], this overlap length will result in delamination of the adherend. The specimens tested for this overlap length have the same layout as the ones in 4.1.

The specimens were tested according to standard ASTM D1002-01, in an INSTRON® model 3367 universal test machine with a capacity of 30 kN, at room temperature and constant displacement rate of 1 mm/min. To fix the specimens, two mechanical wedge-action grips (Figure 36.b) were used.

4.2.1 CFRP-only, reference joints

The reference joints were tested in order to establish a baseline for the other tests. The failure of the joints was different. In the case of the 3.2 mm adherend delamination of the substrate occurred (Figure 45.a), while for the 6.4 mm thick substrate a cohesive failure in the adhesive (Figure 45.b) was the mechanism. A reason for the change of the failure mode is the reduction of peel stresses due to the higher longitudinal stiffness of the thick adherends.

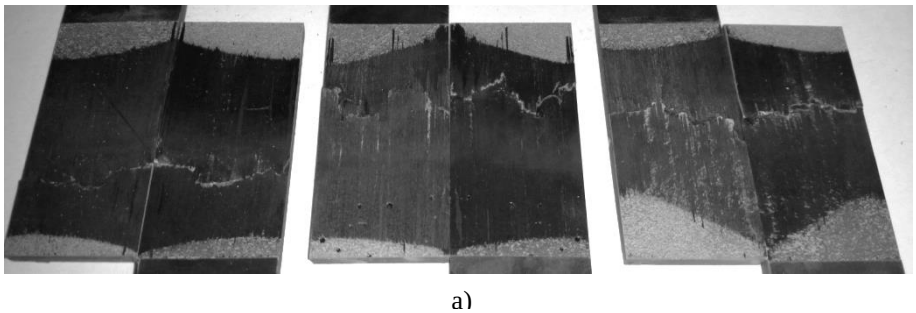

a)

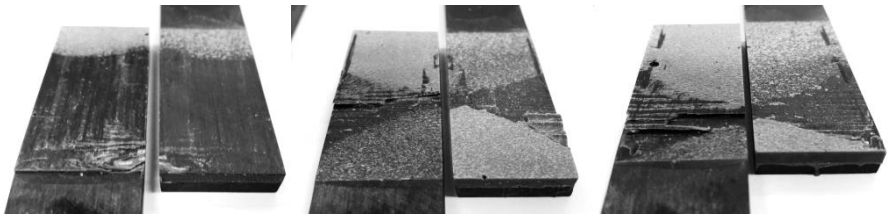

b)

Figure 45 – Failure surface of the reference single lap joints: a) adherend thickness of 3.2 mm; b) adherend thickness of 6.4 mm;

The joint with thicker substrates has higher load bearing capabilities than the one with 3.2 mm thick adherends. The P-δ curves obtained during testing are presented in Figure 46 while the average values are presented in Table 7.

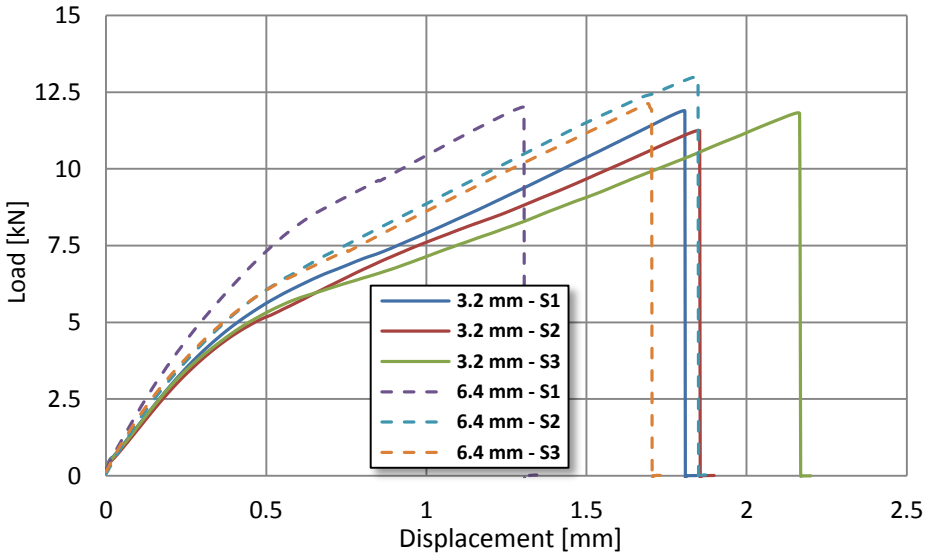

Figure 46 – P-δ curves obtained for reference joints with an overlap of 50 mm

Table 7 – Average failure loads for reference joints with 50 mm overlap

Specimen thickness	Average load [kN]	Failure mechanism
3.2 mm	11.66±0.35	delamination
6.4 mm	12.38±0.54	cohesive

4.2.2 CFRP-Al-CFRP – Type laminate

This laminate exhibited very good properties when tested in three point flexural bending (4.1.2), increasing the maximum load by 7.3% comparing with the reference manufactured of only CFRP. The failure mode of this joint was also delamination (Figure 48) and the maximum load values are slightly higher comparing with the reference joint. The P-δ curves are presented Figure 47.

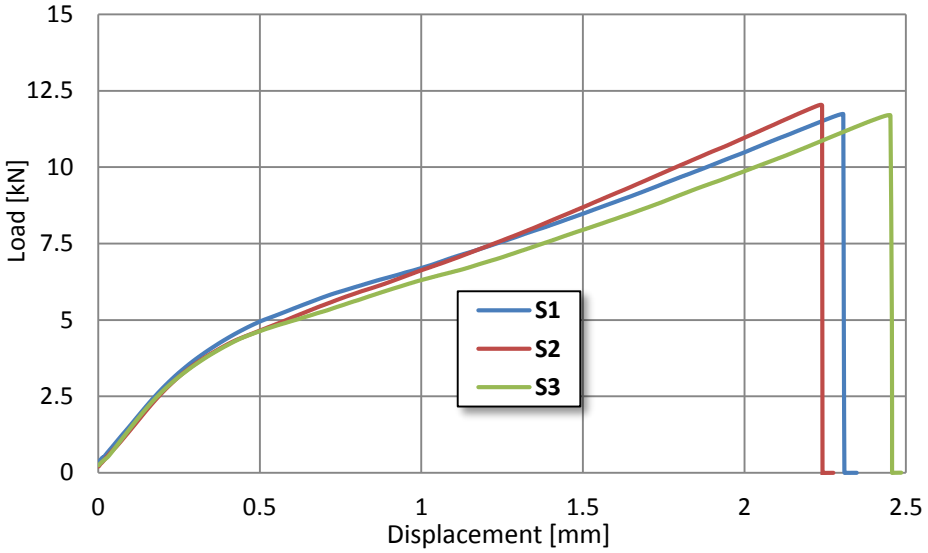

Figure 47 – P-δ curves obtained for CFRP-AL-CFRP – Type joints with an overlap of 50 mm and 3.2 mm adherend thickness

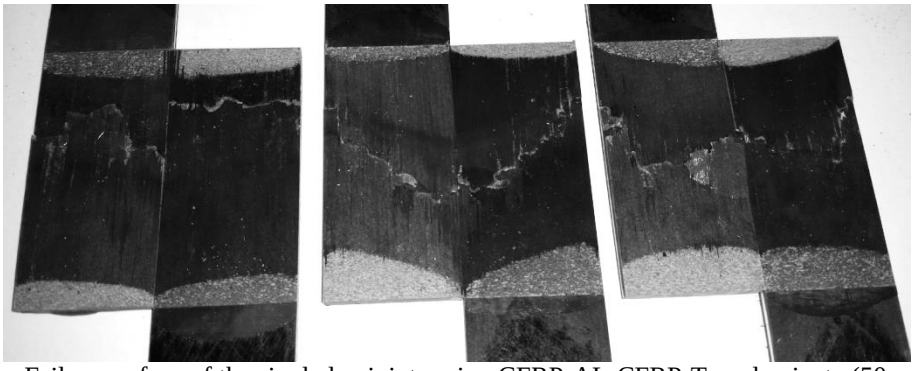

Figure 48 – Failure surface of the single lap joints using CFRP-AL-CFRP-Type laminate (50 mm overlap and 3.2 mm adherend thickness)

The average failure load of these joints was 11.83 ± 0.18 kN which is a marginal increase over the reference joint.

4.2.3 CFRP-AL-CFRP-AL-CFRP – Type laminate

The maximum load achieved using this configuration is slightly higher than the reference joint, scoring an average maximum load of 12.57 ± 0.86 kN; this concludes to a lap shear strength of 10.05 ± 0.69 MPa. This behaviour is normal for a brittle adhesive, for which the increase of the shear area does not provoke the same increase in failure load

[36]. The failure exhibited by this configuration is also cohesive (Figure 49) as it is the one in the reference geometry.

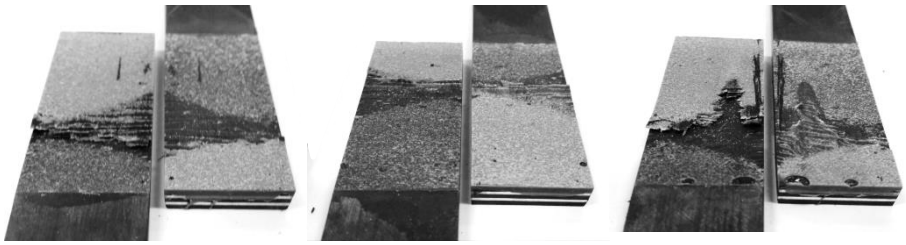

Figure 49 – Failure surface of the single lap joints using CFRP-AL-CFRP-AL-CFRP-Type laminate (50 mm overlap, 6.4 mm adherend thickness)

The P-δ curves of the specimens tested are presented in Figure 50.

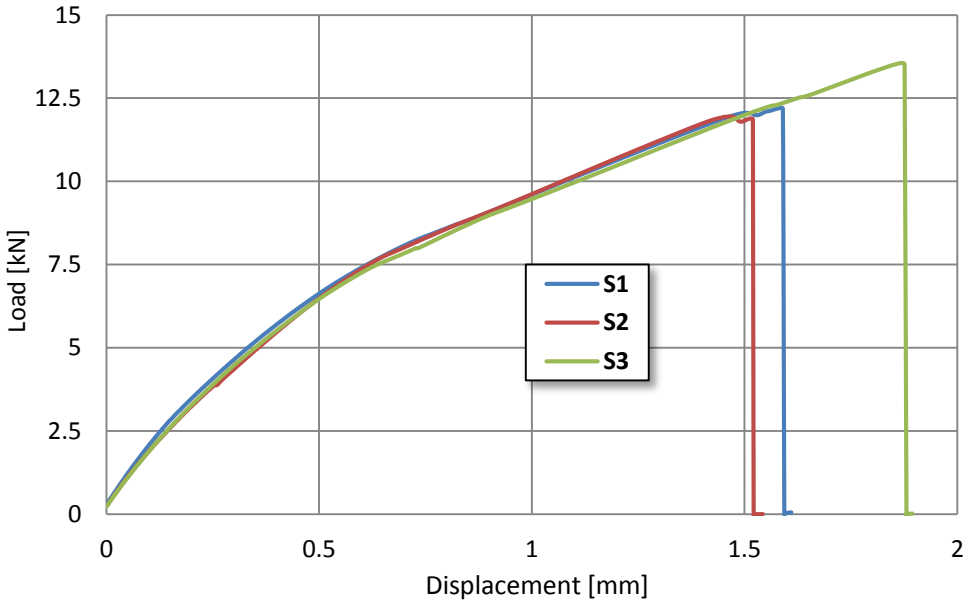

Figure 50 – P-δ curves obtained for CFRP-AL-CFRP-AL-CFRP – Type joints with an overlap of 50 mm and 6.4 mm adherend thickness

4.2.4 AL-CFRP-AL – Type laminate

In the case of the small overlap this laminate had the highest failure load, while for the 50 mm overlap, the load bearing capabilities were lower than the reference. The failure was cohesive near the interface and the fracture surface is presented in Figure 51.

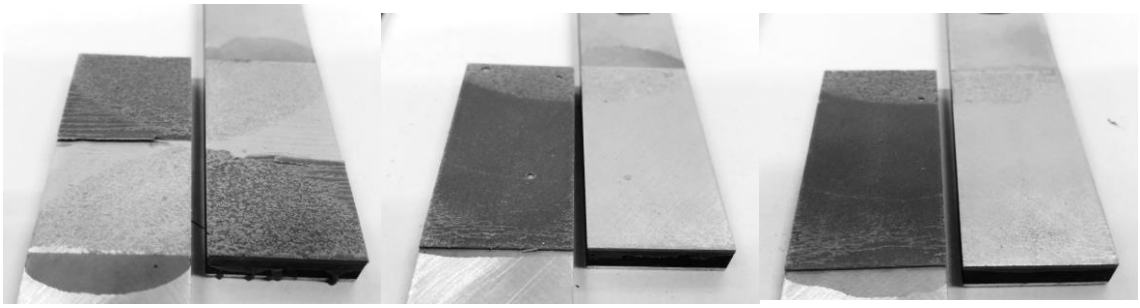

Figure 51 – Failure surface of the single lap joints using AL-CFRP-AL-Type laminate (50 mm overlap, 6.4 mm adherend thickness)

The average failure load recorded for this laminate is 10.84 ± 0.44 kN which leads to a lap shear strength of 8.67 ± 0.352 MPa. The load carrying capability of these joints was the lowest among all the joints tested. This strength reduction could be an effect of the yielding of the aluminium or the shift of the locus of failure. The P-δ curves obtained for this joint configuration are presented in Figure 52.

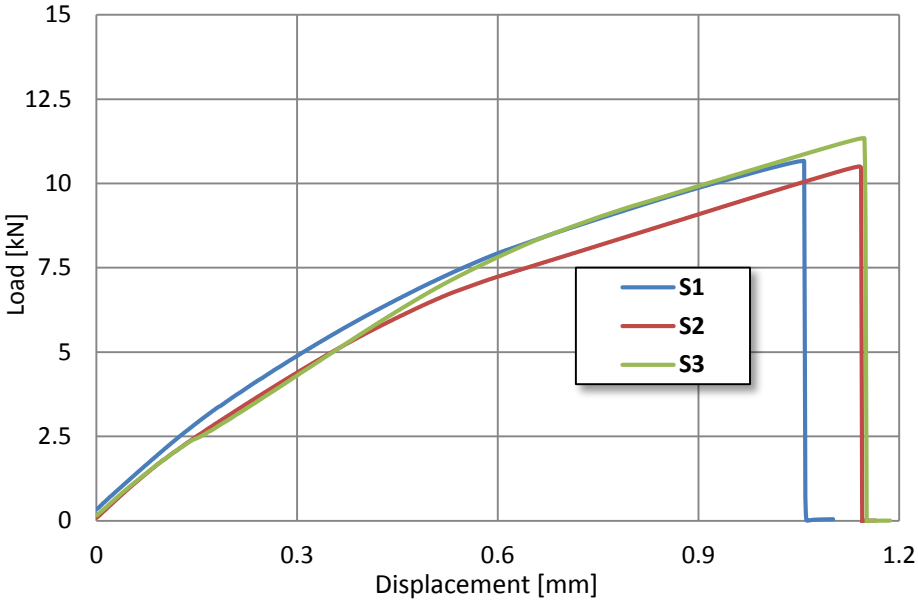

Figure 52 – P-δ curves obtained for AL-CFRP-AL – Type joints with an overlap of 50 mm and 6.4 mm adherend thickness

The cohesive failure near the interface presented in Figure 51.b and c could be due to the length of the overlap and to the higher elasticity of aluminium comparing to CFRP, which leads to high strains appearing at the edge of the joint. In fact the locus of failure in an adhesive joint can be affected by many parameters of the substrates. Chemical and physical properties of adherends influence the crack path through an adhesive [38]. Passivation of the aluminium layer could lead to higher load bearing capabilities of the joint.

4.3 Discussion of the results

4.3.1 Comparison between the joints with the overlap of 12.5 mm

In order to compare the results obtained for this overlap length, a bar chart is depicted in Figure 53. The values are normalized to the value obtained by the reference joint while the absolute failure load values for the joints are presented in Table 8.

Table 8 – Failure load values for the joints with a 12.5 mm overlap

Type	Thickness [mm]	Average load [kN]	Standard deviation	Failure type
	3.2	8.73	0.11	Cohesive
	3.2	8.40	0.21	Cohesive
	6.4	9.20	0.55	Cohesive near the interface
	6.4	8.40	0.83	Cohesive near the interface
	6.4	9.60	0.15	Cohesive near the interface

Increasing the thickness led to a slight increase of the average failure load. This behaviour was expected due to the fact that a thicker adherend has a higher stiffness, therefore the bending of the specimen during testing is lower which leads to lower peel stresses [23] and the adhesive is subjected to more shear stress.

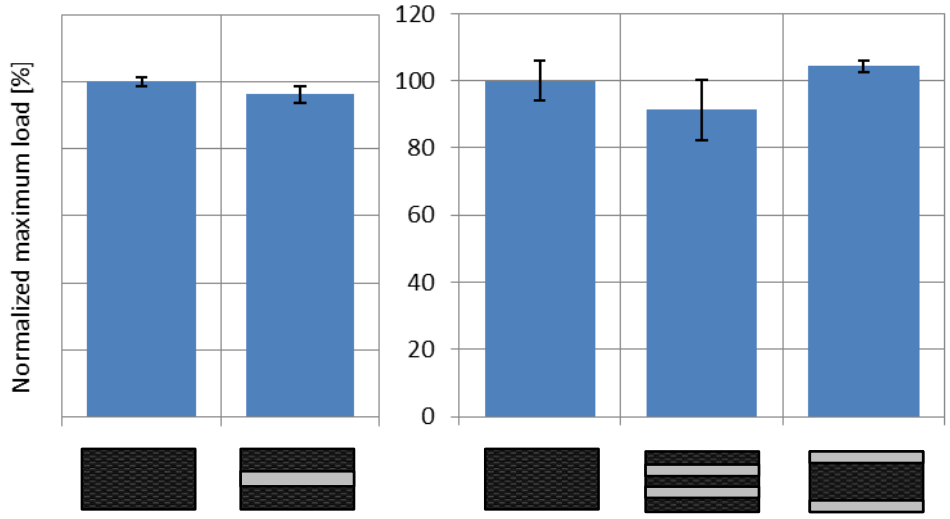

Figure 53 – Comparison between the maximum loads obtained (12.5 mm overlap): adherends with 3.2 mm thickness (left), adherends with 6.4 mm thickness (right)

Considering both adherend thickness, the laminates which had the aluminium in the middle of the laminate, have a lower strength than the reference geometries while the highest joint strength was achieved using the Al-CFRP-Al – type laminate (Figure 16.d).

4.3.2 Comparison between the joints with the overlap of 50 mm

Joints with the overlap of 50 mm were manufactured because, according to Neto, et al. [29], a delamination failure of the adherend was expected. While in the case of thinner adherends, delamination of the CFRP substrate was obtained, in the case of thicker adherends the failure was cohesive. In the next table a summarization of the results is presented.

Table 9 – Failure load values for the joints with a 50 mm overlap

Type	Thickness [mm]	Average load [kN]	Standard deviation	Failure type
	3.2	11.66	0.35	Delamination
	3.2	11.83	0.19	Delamination
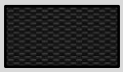	6.4	12.38	0.54	Cohesive
	6.4	12.57	0.86	Cohesive
	6.4	10.84	0.44	Cohesive

In order to evaluate better the results, a bar chart (Figure 54) consisted of normalized values for maximum load is presented. A slight increase in lap shear strength was observed in cases where the aluminium sheets were place in the middle of the laminate (cases CFRP-AL-CFRP and CFRP-AL-CFRP-AL-CFRP); unfortunately the load increase is smaller in both cases than the standard deviation obtained by the reference specimens. In the case of the thinner adherends the failure mechanism is the same as the one of the reference joint, meaning that the unpredictable delamination failure was not substituted with a cohesive failure of the adhesive layer.

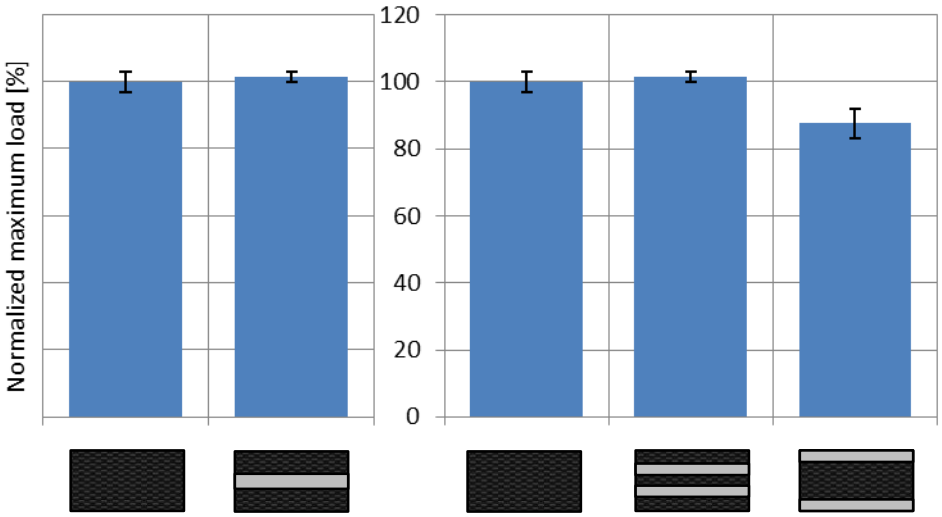

Figure 54 – Comparison between the maximum loads obtained (50 mm overlap): adherends with 3.2 mm thickness (left), adherends with 6.4 mm thickness (right)

In the case of thick adherends the worst behaviour was obtained with the laminate which had the outer surfaces with aluminium (AL-CFRP-AL – Type).

5 Numerical analysis

Nowadays finite element analyses are a powerful tool available to an engineer who needs to evaluate the strength of a designed structure. Finite element software can be used in order to develop a preliminary structure which respects the criteria imposed, eliminating some costly steps needed in a trial-and-error approach.

Because the main objective of this thesis is the optimisation of FML joints, a finite element model was created using the Dassault ABAQUS 6.13 software. In order to reduce the time spent while calculating a solution, 2D static analysis using the implicit solver, was used. The elements used to mesh the model are a 4-node bilinear plane stress quadrilateral element, named CPS4R, utilised for the solid bodies, while the cohesive zone is meshed with a 4-node two-dimensional cohesive element, named COH2D4.

5.1 Thermal stress evaluation

Carbon fibre reinforced plastics have a very low coefficient of thermal expansion in the direction of the fibres, close to 0 [39], while 2024-T3 aluminium alloy, has a linear thermal coefficient of 22.8 $\mu m \cdot m^{-1} \cdot K^{-1}$. The difference between the temperature at which the plate is cured and room temperature conditions is 110°C.

A simple math calculation concludes that the aluminium has to contract from the curing temperature to room temperature conditions, with around 0.75 mm, for an aluminium plate with a length of 300 mm.

To better understand the thermal stresses which led to the buckling (Figure 55) of the configuration depicted in Figure 16.b, a 2D finite element analysis was conducted using ABAQUS 6.13.

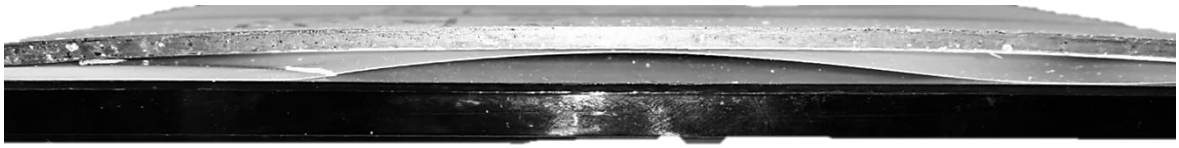

Figure 55 – Buckled plate with the CFRP-Al layup ()

The material properties used for CFRP are the ones determined by Campilho [40] and are presented in Table 10.

Table 10 - CFRP components elastic orthotropic properties for a unidirectional ply [39]

E_x [MPa]	E_y [MPa]	E_z [MPa]	ν_{xy}	ν_{yz}	ν_{xz}	G_{xy} [MPa]	G_{yz} [MPa]	G_{xz} [MPa]
109000	8819	8819	0.342	0.342	0.380	4315	4315	3200

The finite element analysis is consisted of a simple 2D model, which has the dimensions of a standard substrate for a 50 mm overlap single-lap joint. The elastic properties used for the aluminium alloy are presented in Table 2. A simple mesh consisted of 584 quad elements (4-node bilinear plane stress quadrilateral element was used, named CPS4R) was used (Figure 56.a). The equivalent von Mises stress (Figure 56.b,c) has a maximum value of 209 MPa for the aluminium alloy and 163 MPa for the CFRP in contact with the aluminium.

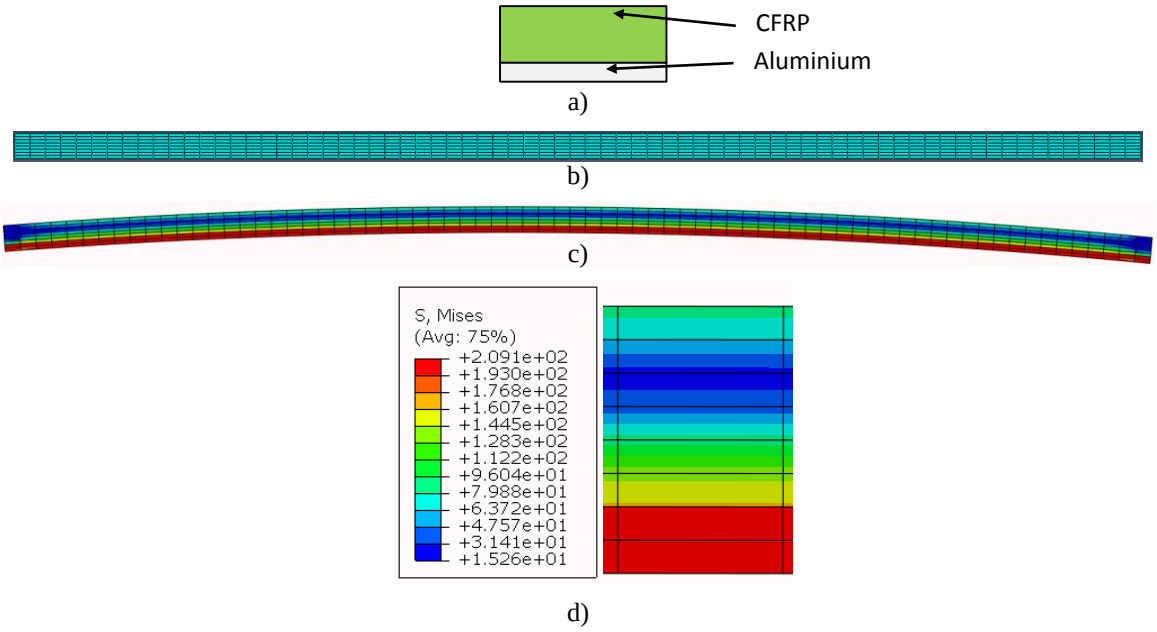

Figure 56 – Thermal stress analysis of the CFRP-Al laminate: a) lay-up of the model b) FEA mesh; c) Equivalent von Mises stress plot (deformed view); d) detail view of von Mises stress plot

The total deformation is consistent to the one of the real plate (Figure 55). This analysis shows that the residual thermal stresses cannot be ignored in future analyses. The stress values due to thermal expansion are high, considering the fact that the yield strength of this alloy is 289MPa.

5.2 Strength prediction

In order to evaluate the strength of the joints, a static finite element analysis was employed, using Dassault Abaqus 6.13. Because of the simple geometry of the joint, 2D models were developed. All models used the same parameters:

- In order to mesh the solid bodies a 4-node bilinear plane stress quadrilateral element was used, named CPS4R;
- In order to mesh the cohesive layers a 4-node two-dimensional cohesive element was used, named COH2D4;

The cohesive law employed is the triangular law available in the software suite (depicted in Figure 15), this law can replicate the behaviour of a brittle adhesive very well.

In order to determine the correct element size, a mesh influence study was conducted. This consisted of running multiple analyses while gradually decreasing the element size until the difference between two subsequent results is less than 3%.

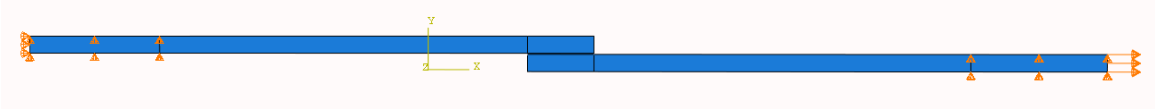

Figure 57 – Boundary conditions used

The boundary conditions were consistent in all the simulations and they are depicted in Figure 57. The left end of the joint was fixed while in the right end a displacement was applied to replicate the loading and the joint was restrained transversely.

5.2.1 CFRP reference joint (3.2 mm thickness) with an overlap of 12.5 mm

A finite element analysis of the SLJ with the overlap of 12.5 mm was used, in order to develop a more complex model that can be used to predict the strength of the joints studied in this thesis. The main objective of this FEA is to confirm the data cohesive properties of the AV138M1/HV998 adhesive.

The cohesive properties for the adhesive used are presented in Table 1 while the carbon fibre properties are presented in Table 10.

Loading of the specimen is done by imposing a 3 mm displacement to the right end of the joint. Because in the case of the real joint tested no delamination occurred, in the case of the simulation the carbon fibre was modelled as homogenous material without any cohesive zone elements. The mesh used consisted of 924 elements, with the adhesive bond being reproduced using 40 elements with progressive size. A detail view on the mesh used is represented in the Figure 58.

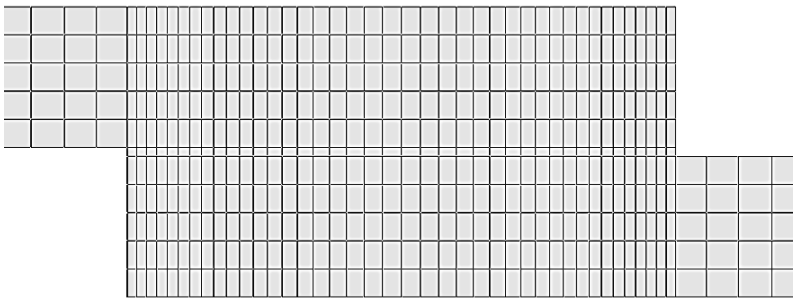

Figure 58 – Detail view of the mesh used to model the SLJ with 12.5 mm overlap

The results obtained (Figure 59, Figure 60) correlate very well to the results obtained while testing the same reference joint. The only difference is the displacement which does not have the same value due to the slippage of the grips on the specimen.

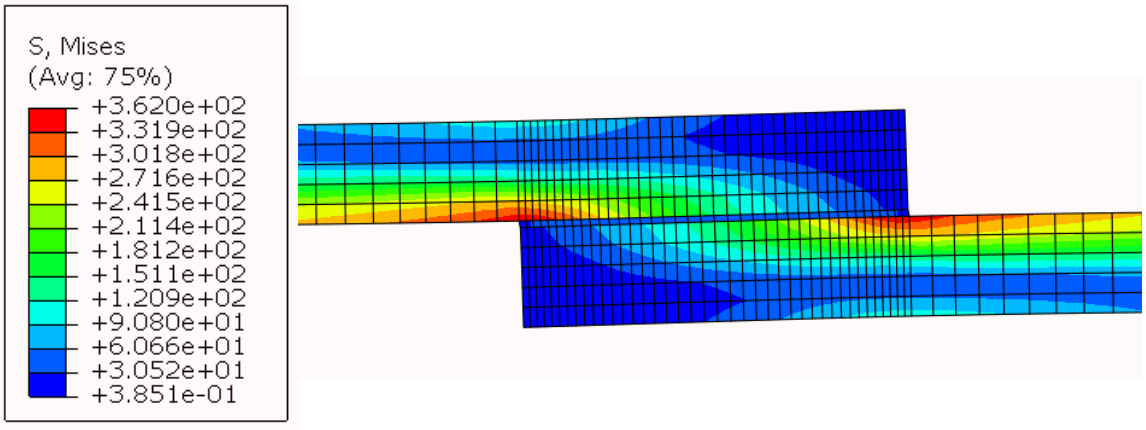

a)

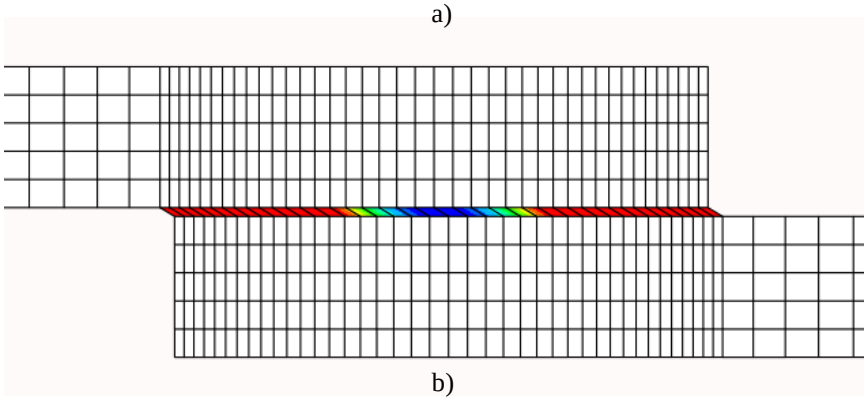

b)

Figure 59 – a) von Mises stress plot, before the failure of the adhesive; b) degradation of the adhesive

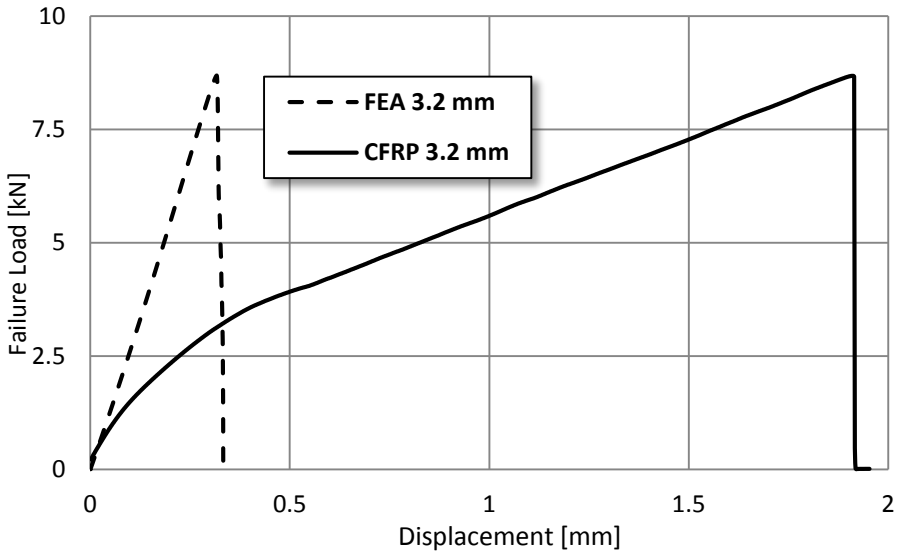

Figure 60 – Comparison of P-δ curves obtained experimentally and using FEA

The FEA calculated a maximum load of 8.69 kN, while the experimental tests gave the value of 8.72 ± 0.11 kN; the error obtained was -0.34%. This reveals that the properties of the adhesive are correct.

5.2.2 CFRP reference joint (3.2 mm thickness) with an overlap of 50 mm

After the validation of the properties of the adhesive, a new simulation was done in order to validate the cohesive properties of the CFRP obtained by Campilho [40]. The cohesive properties used are presented in the Table 11.

Table 11 – Interlaminar cohesive properties of CFRP [39]

Parameter	Value
σ_u [MPa]	25.0
τ_u [MPa]	13.5
G_{IC} [N/mm]	0.33
G_{IIC} [N/mm]	0.79

In order to properly simulate the delamination process, a cohesive element layer (0.02 mm thick) was introduced in the substrate, at a distance of 0.05 mm from the adhesive layer. Detail views of the joint can be observed in Figure 61. The loading and the boundary conditions are identical to the ones used in 5.2.1.

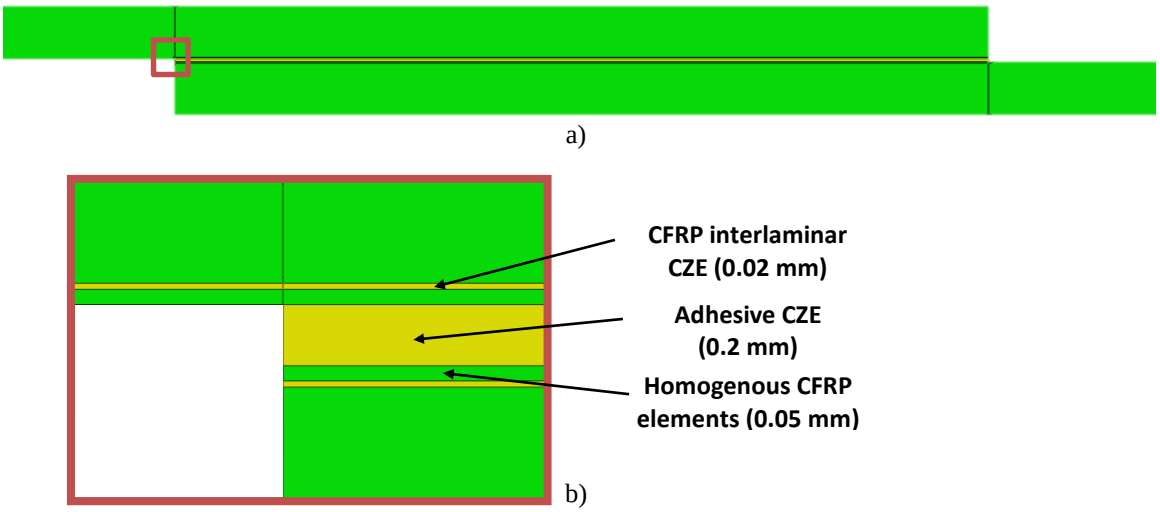

Figure 61 – a) Detail view on the joint with 50 mm overlap; b) Enlarged detail view in which the CZE layers can be observed

The simulation replicated the results obtained experimentally. The cohesive zone elements placed between the layers of carbon fibre were damaged similar to the experimental case, and the plot of element degradation is presented in Figure 62.b.

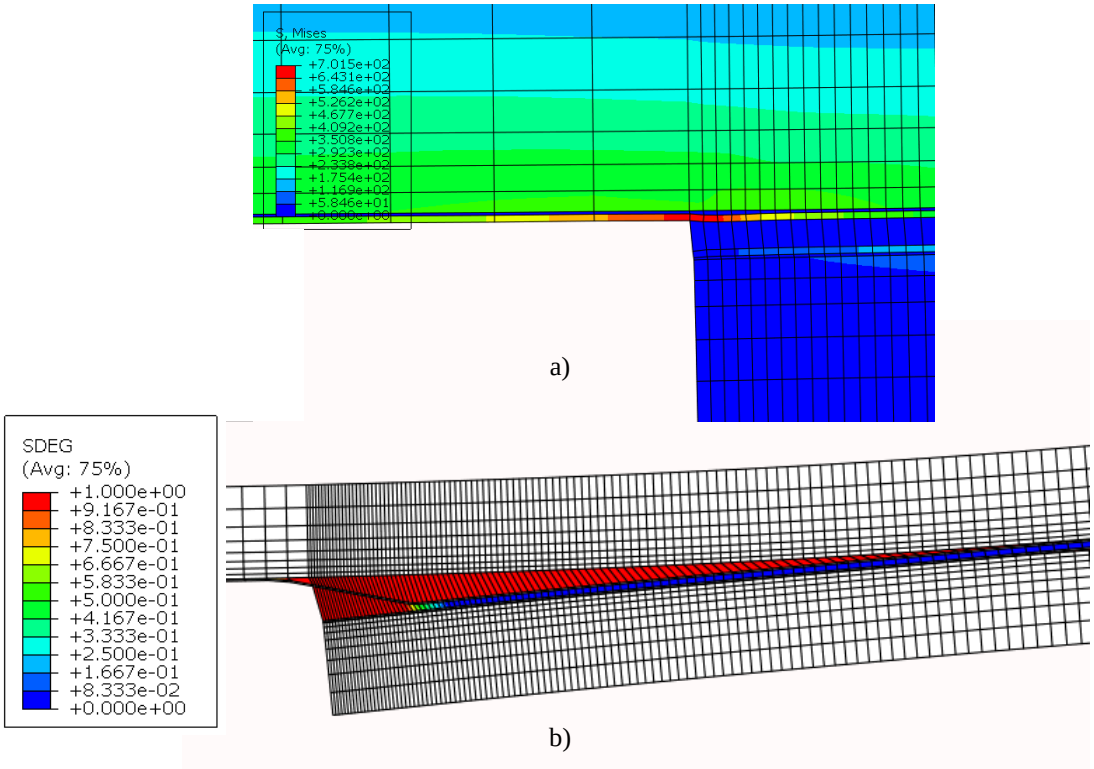

Figure 62 – CFRP reference joint with 50 mm overlap length and 3.2 mm adherend thickness; a) Von Mises stress plot on the detail view of the delamination zone; b) Degradation of the cohesive zone elements

The stress values in the first lamina (Figure 62.a) are very high and would lead to a fibre failure.

The traction separation law is composed of a linear elastic section, which corresponds to a gradual loading until the stress criterion is achieved, followed by a softening phase, which uses fracture mechanics. The latter part of the law corresponds to the damage of the simulated material and is irreversible. In case of the law implemented in ABAQUS®, this means that if unloading occurs, subsequent loading will not follow the initial path along the linear elastic of the undamaged model, but one that has the end point in the place where unloading occurred. The degradation of an element is a measure of how much softening the element was subjected to. If we analyse the degradation of the cohesive zone elements we can observe that the failure mode is very similar to the one of the real joints (Figure 46). At the edges it is cohesive failure of the adhesive, and then the crack path jumps to one of the adherends. The fracture changes from one adherend to the other at the middle of the joint, and then the joint fails. The P-δ curves comparing the numerical simulation to the real single lap joint are presented in Figure 63.

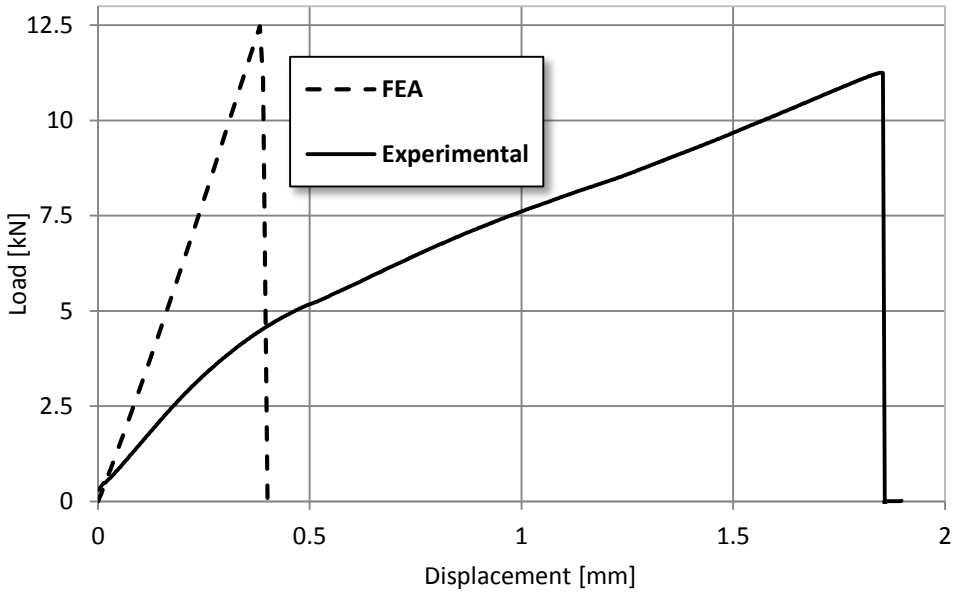

Figure 63 – Comparison of P-δ curves between FEA and experimental (50 mm overlap, 3.2 mm adherend thickness)

The maximum load obtained in the finite element analysis is 12.47 kN while the real joints have an average maximum load of 11.66 ± 0.35 kN, this leads to an error of 6.94% which can be considered as a very accurate model.

5.2.3 CFRP Reference joint (6.4 mm thickness) with 12.5 mm overlap

In order to verify that the model is not affected by the increase of the adherend thickness and subsequently by the increase in longitudinal stiffness, a model was created to verify the validity of the model.

The mesh was adapted to the bigger volume of the thicker adherends in order to better capture the local effects at the ends of the joint overlap.

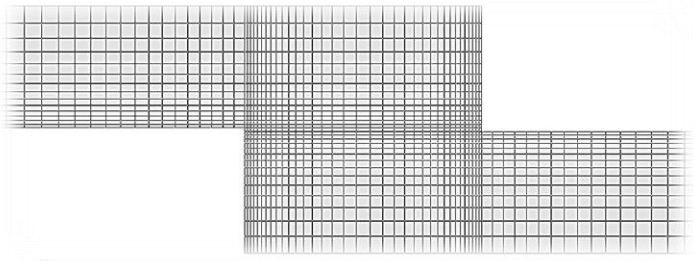

Figure 64 – Detail view on the mesh used for the numerical analysis of the thicker adherends (12.5 mm overlap)

Because of the increased longitudinal stiffness, the adhesive fails due to general yielding caused by shear stresses; this can be observed in Figure 65.

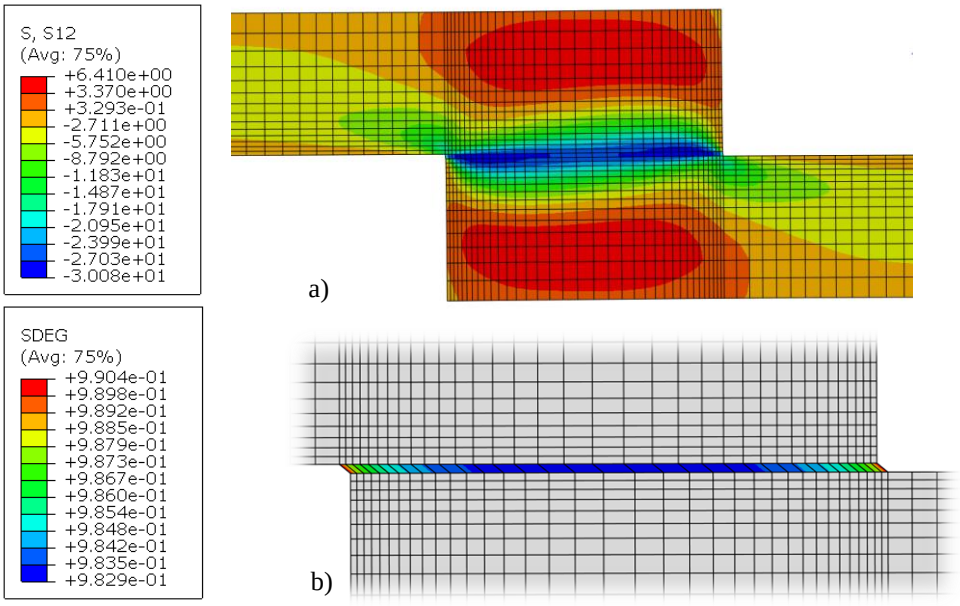

Figure 65 – Representation of: a) the shear stresses, b) element degradation

The P-δ curves comparing the numerical simulation to the real single lap joint are presented in Figure 66.

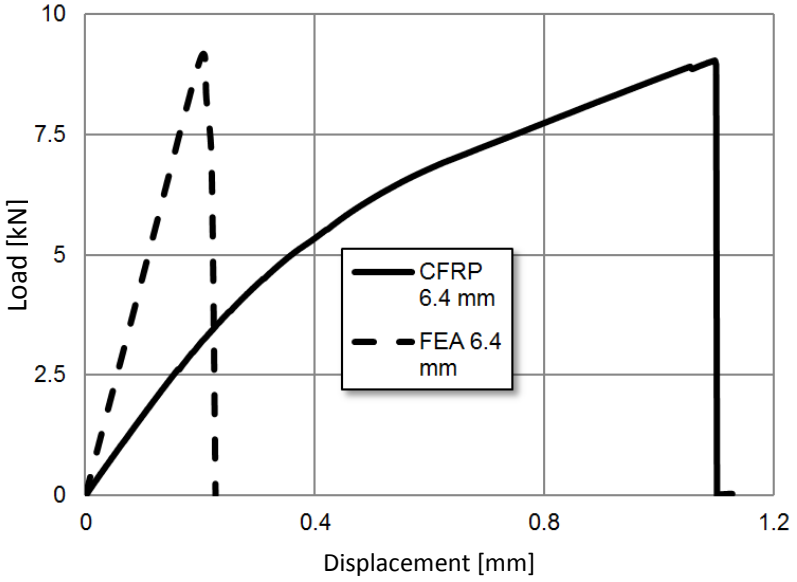

Figure 66 – Comparison of P-δ curves between FEA and experimental (12.5 mm overlap, 6.4 mm adherend thickness)

The maximum load obtained in the finite element analysis is 9.18 kN while the real joints have an average maximum load of 9.196 ± 0.55 kN, this leads to an error of -0.17% which proves that the simulation is very accurate. The difference between the slopes of the two curves is attributed to the slippage of the grips on the experimental test.

5.2.4 CFRP Reference joint (6.4 mm thickness) with 50 mm overlap

Because of the brittle nature of the adhesive used it is essential to calibrate the model on the reference joint with thick adherends and 50 mm of overlap. Because there was no delamination in the experimental test, no cohesive zone elements were introduced in the CFRP. The degradation plot right before the sudden failure of the adhesive is depicted in Figure 67, while in Figure 68 the P-δ curves comparing the numerical simulation to the real single lap joint are presented.

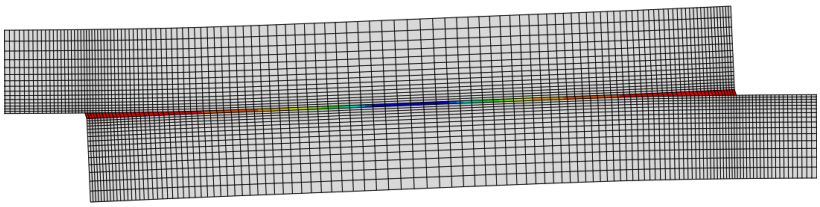

Figure 67 – Representation of the cohesive element degradation for the SLJ with 50 mm overlap and 6.4 mm adherend thickness

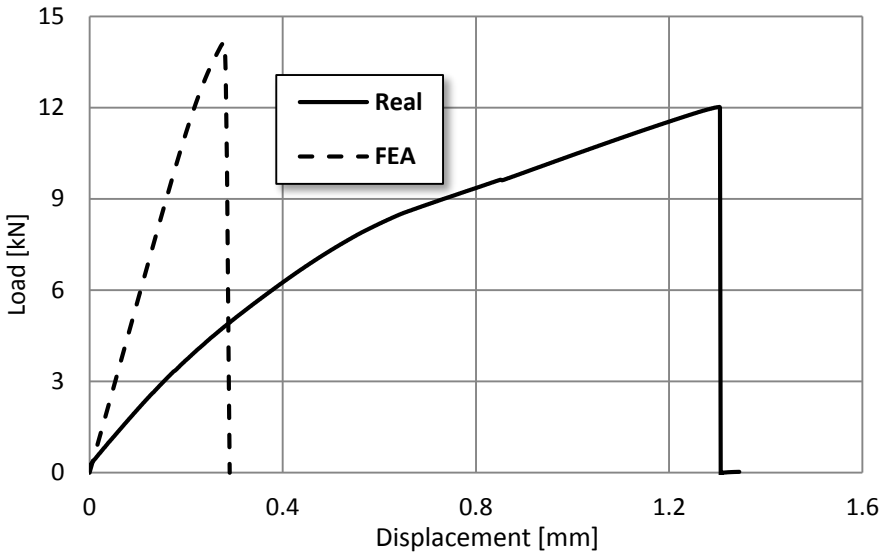

Figure 68 – Comparison of P-δ curves between FEA and experimental (50 mm overlap, 6.4 mm adherend thickness)

This numerical simulation returned a maximum load value of 14.079 kN, which compared to the experimental results of 12.38 ± 0.54 kN, gives an error of 13.72% which is not a very good result but could be considered satisfactory.

5.2.5 Conclusions regarding the strength prediction of the single lap joints

The finite element model developed using ABAQUS® reproduces very well the behaviour of the joints which were tested experimentally. As it was shown in section 5.2.2 the delamination phenomena can also be replicated using this model and the numerical results are trustworthy. In order to analyse the accuracy of the model, two graphs, which compare the influence of the overlap length for the reference joints are presented (Figure 69).

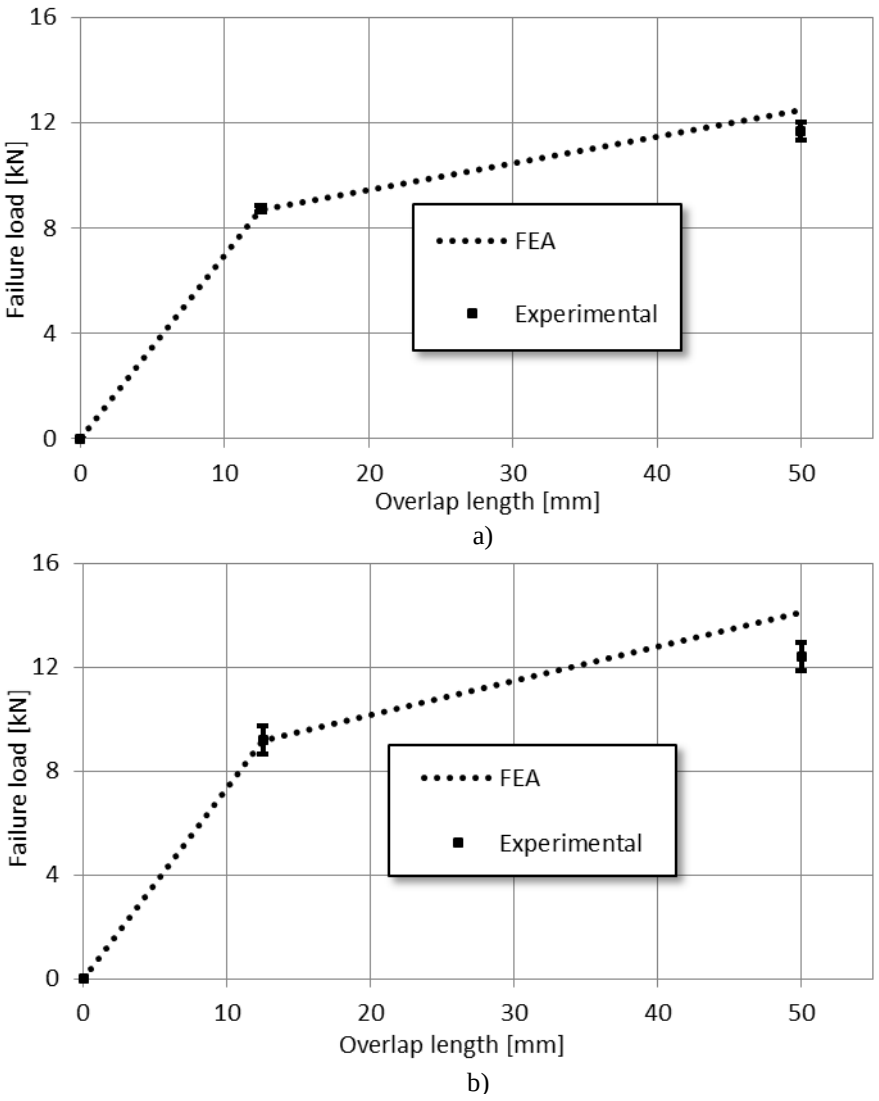

Figure 69 – Influence of the overlap length on the strength of the joint: a) 3.2 mm thick adherends, b) 6.4 mm thick adherends

In the case of a brittle adhesive, an increase in lap shear area does not translate into the same increase of the load bearing capacity of the joint [37]. The finite element model replicates the results obtained experimentally with great accuracy. In the case of 12.5 mm overlap, the predicted value is very precise while for the large overlap the value returned by the analysis is slightly higher.

The behaviour shown is typical for simulations which use brittle adhesives with cohesive zone models This combination makes the softening process more abrupt which, in addition to the smaller fracture process zone at the crack tip, might cause some discrepancies between experimental and numerical data [24].

The model used to simulate the reference joints, was found to be accurate enough and as a consequence, numerical simulations were undertaken on all the joints studied. Due

to the results obtained in section 3.4, regarding the cohesive properties of the interface between aluminium and CFRP, the model did not account for the possibility of debonding in that region. The comparison between numerical and experimental results, is presented in Figure 70.

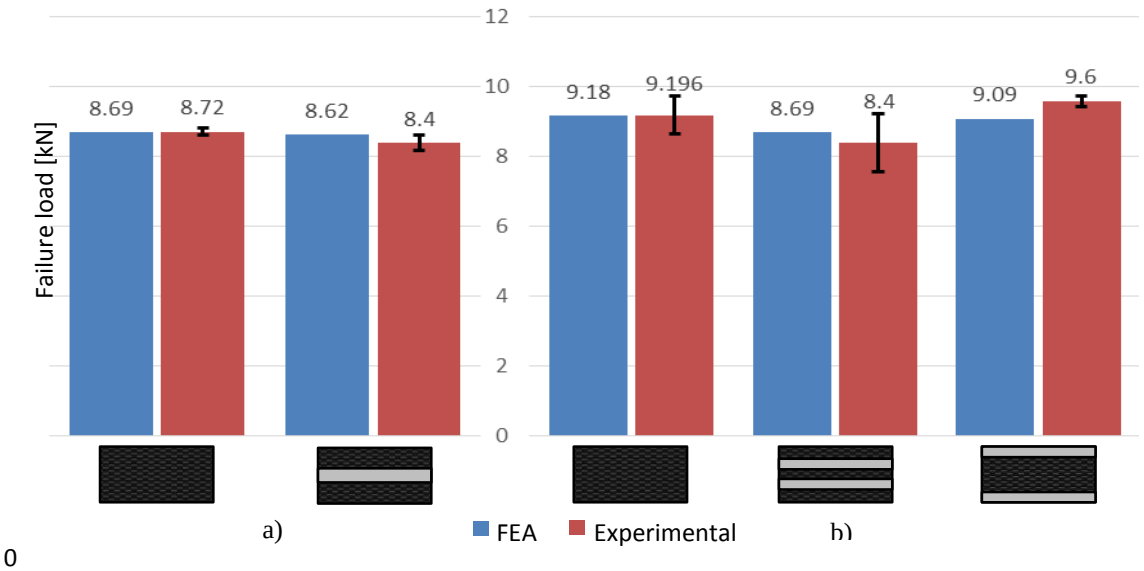

Figure 70 – Comparison between experimental and numerical results for the joints with 12.5 mm overlap, a) 3.2 mm adherend thickness, b) 6.4 mm adherend thickness

The finite element analysis returned results which correlate very well with the experimental results. The maximum relative error is 5.3% in the case of Al-CFRP-Al type laminate, in most of the cases the numerical prediction fits within the standard deviation of the experimental values.

Numerical predictions on the joints with an overlap of 50 mm were also studied and a comparison is presented in Figure 71.

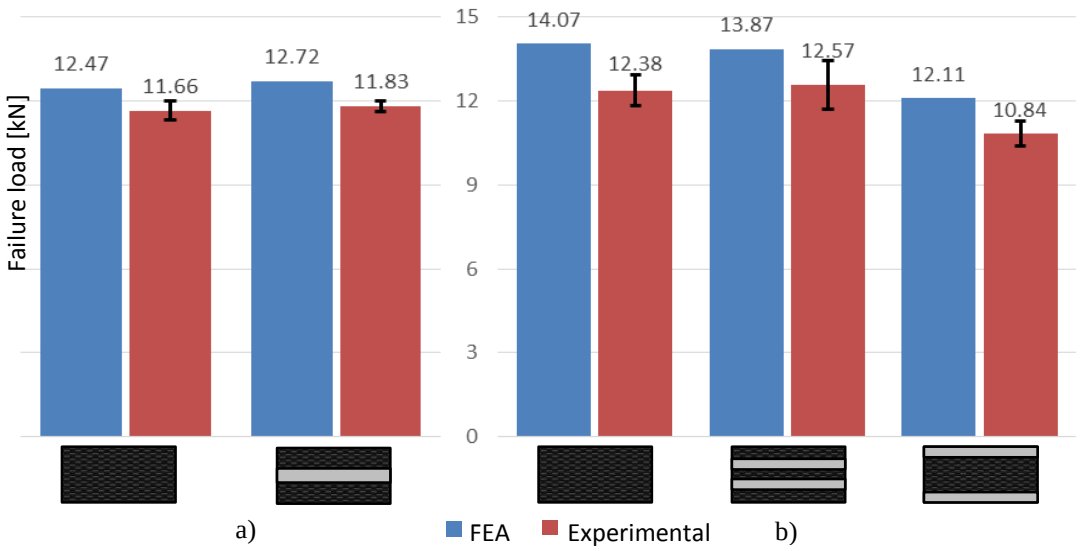

Figure 71 – Comparison between experimental and numerical results for the joints with 50 mm overlap, a) 3.2 mm adherend thickness, b) 6.4 mm adherend thickness

In the case of the joints with an overlap of 50 mm the FEAs also predicted the failure mode of the laminates. The joints which have adherends with the thickness of 3.2 mm exhibited delamination while for the joints with thick adherends, a cohesive failure of the adhesive layer was observed.. The maximum relative error is 13.6% for the thick reference joint. The model is more accurate in predicting the joint strength, when delamination of the substrates can be observed; the numerical value being always higher than the experimental one.

The numerical results correlate very well with the experimental ones and as a consequence, the model can be used in order to study laminate types which were not manufactured and tested.

5.3 Optimization of CFRP joints

The main objective of this thesis is the identification of a joint or adherend configuration using an approach similar to fibre metal laminates, which increases the strength of the CFRP adherends. Because aluminium alloy sheets with the thickness of 0.4 mm could not be found in stock during this study at any of the traditional suppliers, a finite element model will be used to evaluate joints using Al-CFRP-Al laminates which make use of sheets of aluminium with a thickness of 0.4 mm. Different configurations will be simulated using finite element analysis software and the model validated in chapter 5.2.

5.3.1 AL-CFRP-AL – Type with adherend thickness of 3.2 mm and 50 mm overlap length

A finite element analysis was employed in order to evaluate the properties of "AL-CFRP-AL – Type" adherend which has total thickness of 3.2 mm. This laminate uses aluminium with a thickness of 0.4 mm. In order to obtain a good approximation of the behaviour of the joint, the model validated in section 5.2 was used. The laminate structure is presented in Figure 72.

As a consequence of the high thermal stresses induced by the curing process a two-step analysis was used, in order to take in consideration the pre-existing stresses.

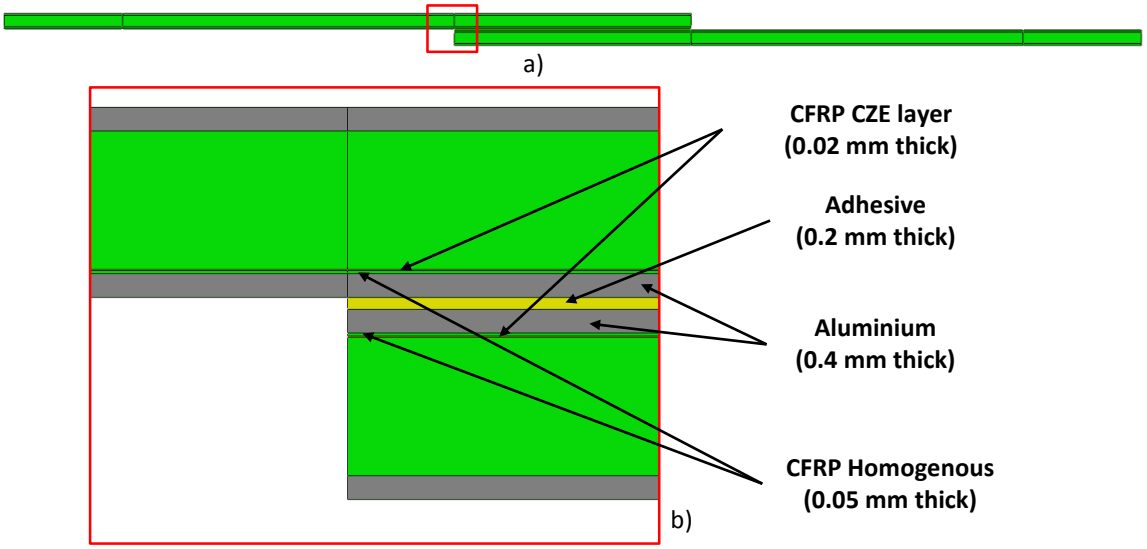

Figure 72 – AL-CFRP-AL – Type laminate structure; a) whole model, b) detail view

The von Mises equivalent stresses induced, only by the contraction of the aluminium are represented in Figure 73.

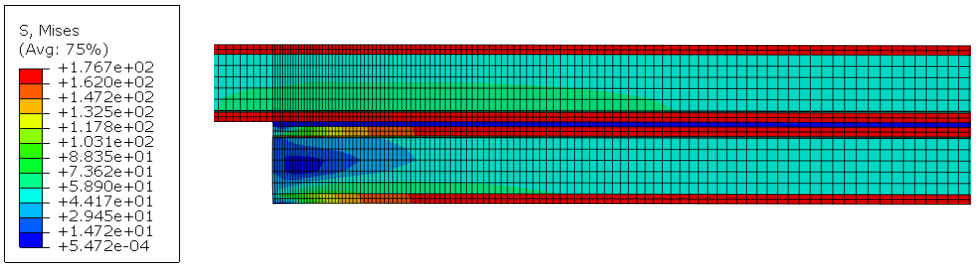

Figure 73 – Pre-existing thermal stresses (detail view of the overlap)

The idea of this laminate is that the isotropic layer of aluminium will distribute the peel stress over a larger area than a CFRP Layer would do. The element degradation plot is presented in Figure 74.

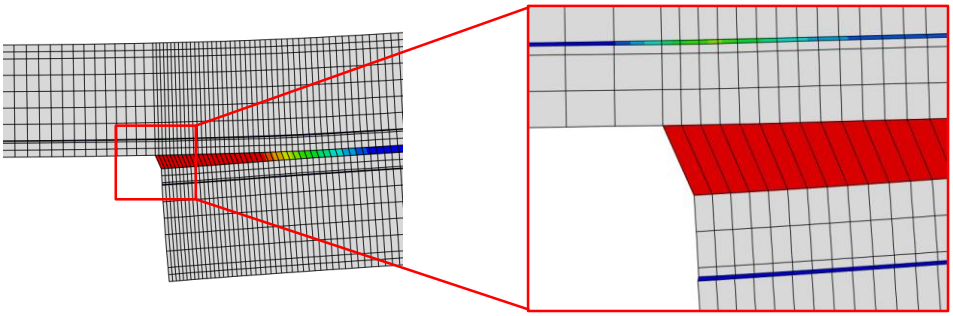

Figure 74 – Detail view of the element degradation

Figure 74 shows that the failure of the joint is due to a cohesive failure of the adhesive layer and not due to the failure of the cohesive layer introduced in order to simulate the delamination of the carbon fibre reinforced plastic. In addition to the improved failure mode, the joint strength increased from the reference load of 11.66 ± 0.35 kN obtained for substrates manufactured only with CFRP to 13.29 kN, leading to a 13.94% increase in load bearing capabilities.

5.3.2 AL-CFRP-AL – Type approach with shorter aluminium overlap

One of the advantages of using fibre reinforced plastics is the ability to form them in the shape needed. Having a laminate designed after the AL-CFRP-AL – Type is not so easy to manufacture in more complex shapes.

The next design of the laminate will try to evaluate the feasibility of using a fibre metal laminate only in the bond area. Because of the high peel stresses which appear at the end of the overlap area, the sheet used will be with 50% longer than the overlap. A graphic representation of the joint is given in Figure 75.

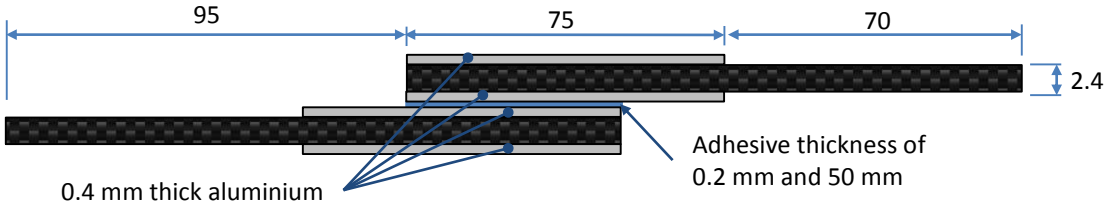

Figure 75 – Alternative joint design for the AL-CFRP-AL – Type structure

The residual stresses due to the cure process of the laminate have high levels and are depicted in Figure 76.

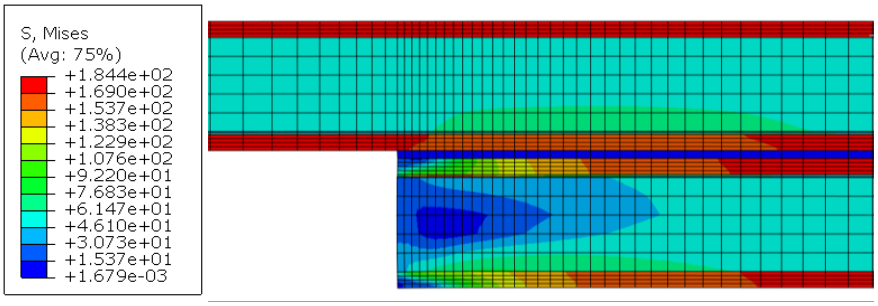

Figure 76 – Equivalent stress due to the contraction of the aluminium alloy sheet

This solution exhibited a good behaviour in the finite element analysis the failure mode of the joint being cohesive in the adhesive layer, while the joint strength comparing with the reference joint, increased by 9.1% to the value of 12.72 kN. Nevertheless there is some marginal damage in the cohesive zone elements used to model the interlaminar properties of the CFRP, this is depicted in Figure 77.

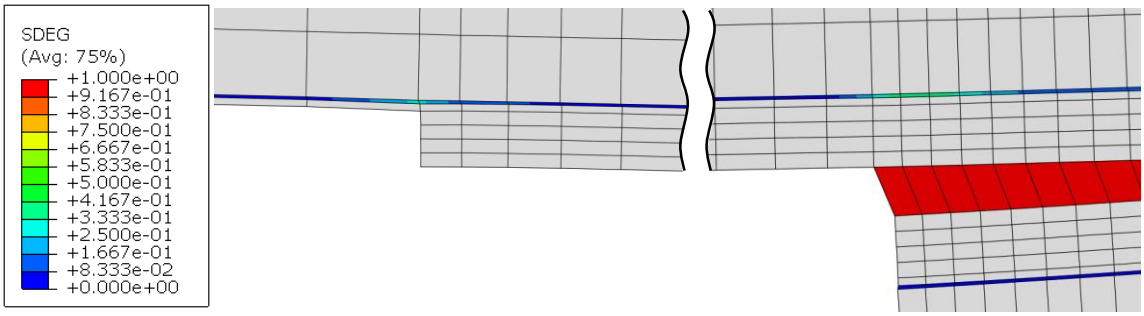

Figure 77 – Detail view on the element degradation of the alternative design

The damage present in the cohesive zone of the carbon fibre reinforced plastics is higher at the end of the adhesive overlap than at the end of the aluminium reinforcement. The value recorded for the damage is around 40% at the end of the overlap and as low as 20% at the end of the reinforcement.

6 Conclusions

The main objective of this study was the optimisation of CFRP joints using fibre metal laminates. In order to accomplish this goal, the influence of surface treatment on the bond properties between the aluminium metal sheet and the CFRP was studied experimentally, also experimental tests and numerical simulations were conducted, to evaluate the strength of the joints designed.

This study has shown that phosphoric acid anodisation is the best surface treatment to use in order to bond aluminium to a CFRP laminate during the cure process. The adhesion properties obtained this way are better than the adhesive properties between the laminas of the carbon fibre reinforced plastics.

Using thicker adherends higher failure loads can be obtained, because a thicker adherend has a higher longitudinal stiffness which reduces the bending of the adherend and decreases the peel stresses.

The thermal stresses analysis proved that high residual thermal stresses are present in the laminate, due to the very low thermal expansion coefficient of CFRP. The average equivalent von Mises stress is normally, in this setup, higher than half of the yield strength of the aluminium alloy.

This study has shown that laminates that have aluminium in the middle, used in a 50 mm overlap joint, exhibit slightly higher strength values than the reference joints. But the increase in strength is not higher than the standard deviation of the reference joint.

The numerical model developed in ABAQUS® is a good approximation of the joints studied, offering results which can be used to further optimize joints which have not been studied experimentally.

The laminate consisted out of aluminium-CFRP-aluminium, with a thickness of 3.2 mm was studied using the numerical model developed and exhibits good properties. It prevents the delamination of the CFRP, offering an increase in joint strength of 13.94% in comparison with the reference joint. Because the weight to strength ratio is an important parameter in the design of automotive and aeronautical structures, a laminate using the concept of fibre metal laminates only for an area slightly larger than the overlap area, was studied. This laminate can prevent the delamination of the CFRP, increases the joint strength by 9.1% comparing to the reference joint and also facilitates the manufacture of complex structures using fibre reinforced plastics.

7 Future work

During the numerical analysis section of this study a possible solution was found for the assumed goal; as a consequence, the future work should study the properties of these joints. Also other ratios of metal to composite should be studied.

Because the main area of interest for the solutions developed is the aeronautical industry, the mechanical properties of the joints should be evaluated using an aeronautical adhesive.

The high thermal stresses are of concern because of fatigue strength of the structures. In order to improve the fatigue properties, the thermal stresses should be reduced. Because all aluminium alloys have roughly the same thermal expansion coefficient, changing the alloy will not reduce the thermal stress. Another possible material to use, in order to optimise the joint should be titanium Ti-6Al-4V (grade V), which has a CTE of 9.2 $\mu m \cdot m^{-1} \cdot K^{-1}$. In addition to the lower CTE the yield strength of this alloy is around 1100 MPa. Future work regarding the use of this alloy should evaluate the adhesion properties between it and the CFRP and also the joints developed using Ti-6Al-4V.

References

[1] Boeing Company, *Boeing: About the 787 Family*, http://www.boeing.com/boeing/commercial/787family/background.page?, (last accesed: 10 March 2015)

[2] Asundi, A. and Choi Alta, Y.N., *Fiber metal laminates: an advanced material for future aircraft*, J. Mater. Process. Technol., **63**, 384-394 (1997)

[3] da Silva, L. F. M., Adams, R. D., *Techniques to reduce peel stresses in adhesive joints with composites,* Int. J. Adhes. Adhes. **27**, 227-235 (2007)

[4] Koh, T. M., Feih, S., Mouritz, A. P., *Strengthening mechanics of thin and thick composite T-joints reinforced with z-pins*, Compos. Part. A-Appl. S., **43**, 1308-1317 (2012)

[5] Ucsnik, S., Scheerer, M., Zaremba, S., Pahr, D. H., Experimental investigation of a novel hybrid metal-composite joining technology, Compos. Part. A-Appl. S., **41**, 369-374 (2012)

[6] Alderliesten, R. C., Benedictus, R., *Fiber/metal composite technology for future primary aircraft structures,* (Conference procedings, Honolulu) 48th Aiaa / Asme / Asce / Ahs / Asc structures, structural dynamics, and materials conference 15th, (2007)

[7] Sinmazçelik, T., Avcu, E., Bora, M. Ö., Çoban, O., *A review: Fibre metal laminates, background, bonding types and applied test methods,* Mater. Design. 7 **32**, 3671-3685, (2011)

[8] Schijve, J., Vogelesang, L. B. and Marisen, R**.,** *Laminate of aluminum sheet material and aramid fibers (US Patent US4500589 A),* (1983)

[9] Wang, W. X., Takao, Y.,Matsubara, T., *Galvanic corrosion-resistant carbon fiber metal laminates (Conference procedings, Kyoto),* ICCM-16, (2007)

[10] Kinloch, A. J., *Adhesion and Adhesives; Science and Technology*, (Chapman and Hall, London, 1987), pp. 1

[11] Adams, R. D., Comyn, J., Wake, W.C., *Structural adhesive joints in engineering,* (Chapman and Hall, London, 1997), 2nd ed.

[12] Stoicescu, A. P., *Proiectarea performantelor de tractiuni si de consum ale automobilelor,* (Ed. Tehnica, Bucharest, 2007)

[13] FEICA, *The Magic World of Adhesives and Sealants (Brochure),* Brussels (2011)

[14] Omar, M. A., *The Automotive Body Manufacturing Systems and Processes,* (John Wiley & Sons, West Sussex, 2011), 1st ed., Chap. 3, pp. 144-149

[15] BMW AG, *The all new BMW 7 Series. All you need to know (Press release),* (2015)

[16] Park, S. Y., Choi, W. J., Choi, H. S., Kwon, H., Kim, S. H., *Recent trends in surface treatment technologies for airframe adhesive bonding processing: a review (1995–2008),* J. Adhesion **86**, 192-221 (2010)

[17] Modern Airliners, *Modern Airliners - Boeing 787 Dreamliner-Specs (website),* (last accesed: 10 March 2015)

[18] Norris, G, *787 Fire Repair Boosts Composites Confidence*, Aviation Week & Space Technology, (2014)

[19] Banea, M. D., Silva, L. F. M., *Adhesively bonded joints in composite materials: an overview*, IMechE **223**, (2008)

[20] Davis, M. J., Bond, D. A., *The importance of failure mode identification in adhesive bonded aircraft structures and repairs*, Directorate General of Technical Airworthiness - Royal Australian Air Force, (2012)

[21] da Silva, L. F. M., das Neves, P. J. C., Adams, R. D., Spelt, J. K., *Analytical models of adhesively bonded joints—Part I: Literature survey,* Int. J. Adhes. Adhes. **29**, 319-330 (2009)

[22] Volkersen, O., *Die nietkraftverteilung in zugbeanspruchten Nietverbindungen mit konstanten laschenquerschnitten,* Luftfahrtforschung **15** (1938)

[23] Goland, M., Reissner, E., *The Stresses in Cemented Joints,* J. Appl. Mech. **11**, A17-A27 (1944)

[24] da Silva, L. F. M., Campilho, R. D. S. G., *Advances in Numerical Modelling of Adhesive Joints*, SpringerBriefs in Applied Sciences and Technology, pp 1-93 (2012)

[25] Adams, R. D., Harris, J.A., *The influence of local geometry on the strength of adhesive joints,* Int. J. Adhes. Adhes **7**, 69-80 (1987)

[26] Adams, R. D., *Adhesive bonding,* (Woodhead Publishing Limited, 2005)

[27] Ortiz, M., Pandolfi, A., *Finite-deformation irreversible cohesive elements for three-dimensional crack-propagation analysis*, Int J Numer Meth Eng, **44**, 1267-1282 (1999)

[28] Chandra, N., Li, H., Shet, C., Ghonem, H., *Some issues in the application of cohesive zone models for metal-ceramic interfaces,* Int J Solids Struct, **39**, 2827-2855 (2002)

[29] Neto, J.A.B.P., Campilho, R.D.S.G., da Silva, L.F.M., *Parametric study of adhesive joints with composites, ,* Int. J. Adhes. Adhes., **37**, 96-101 (2012)

[30] da Silva, L. F. M., de Magalhaes, F. A. C. R. G., Chaves, F. J. P., de Moura, M. F. S. F., *Mode II Fracture Toughness of a Brittle and a Ductile Adhesive as a Function of the Adhesive Thickness,* J Adhesion, **86**, 891-905 (2010)

[31] Huntsman Advanced Materials, *Araldite® AV 138M-1 / Hardener HV 998 (Product specifications),* (2012)

[32] Alcoa Mill Products Inc., *Alloy 2024 Sheet and Plate (product specifications),* (last accessed 15 June 2015)

[33] Marceau, J. A., Firminhac, R. H., Moji, Y. *Method for providing environmentally stable aluminum surfaces for adhesive bonding and product produced (Patent),* (1978)

[34] Boeing Company, *BAC-5555 - Phosphoric Acid Anodizing of Aluminium for structural bonding (company standard),* (2001)

[35] ASTM International, *D 3933 - Standard Guide for Preparation of Aluminium Surfaces for Structural Adhesives Bonding (Phosphoric Acid Anodizing)*, (1998)

[36] ASTM International, *D790 - Standard test methods for flexural properties of unreinforced and reinforced plastics and electrical insulating materials*

[37] da Silva, L. F. M., Ramos, J. E., Figueirdo, M. V., Strohaecker, T. R., *Influence of the Adhesive, the Adherend and the Overlap on the Single Lap Shear Strength,* Journal of Adhesion and Interface, **7**, (2006)

[38] da Silva, L.F.M. , Öchsner, A., Adams, R.D., *Handbook of Adhesion Technology,* (Springer, Berlin, 2011)

[39] Ahmed, A., Tavakol, B., Das, R., Joven, R., Roozbehjavan, P., Minaie, B., *Study of Thermal Expansion in Carbon Fiber Reinforced Polymer Composites (Conference procedings),* SAMPE International Symposium, (2012)

[40] Campilho, R. D. S. G., *Repair of Composite and Wood Structures (PhD Thesis),* FEUP, (2009)

[41] Dassault Systemes, *Abaqus Documentation 6.14,* (2014)

[42] Vogelesang, L. B., Vlot, A., *Development of fibre metal laminates for advanced aerospace structures,* J Mater Process Tech, **103**, 1-5 (2000)